Electronic Supplementary Information

An iridium(III) 3-chloro-6-thio-1,2,4,5-tetrazine complex for cysteine conjugation, bioimaging and photoactivated therapy

Lili Huang,[a] Justin Shum,[ab] Lawrence Cho-Cheung Lee,[a] Guang-Xi Xu,[a] Peter Kam-Keung Leung[ac] and Kenneth Kam-Wing Lo*[ac]

[a] Department of Chemistry, City University of Hong Kong, Tat Chee Avenue, Kowloon, Hong Kong, P. R. China; E-mail: bhkenlo@cityu.edu.hk.

[b] Laboratory for Synthetic Chemistry and Chemical Biology Limited, Units 1503-1511, 15/F, Building 17 W, Hong Kong Science Park, New Territories, Hong Kong, P. R. China.

[c] State Key Laboratory of Terahertz and Millimetre Waves, City University of Hong Kong, Tat Chee Avenue, Kowloon, Hong Kong, P. R. China.

Table of Contents

Experimental Section S6

Table S1 Electronic absorption spectral data of complexes **1** – **4** in CH_3CN at 298 K. S29

Table S2 Singlet oxygen ($^1O_2$) quantum yields (Φ_Δ) of complexes **1** – **4** and conjugate **1-RGD** in aerated CH_3CN at 298 K (λ_{ex} = 450 nm). S30

Table S3 Cellular uptake of conjugate **1-RGD** and complexes **2** – **4** in U87-MG, MCF-7 and HEK293 cells without or with pretreatment of RGD peptide (50 μM, 30 min). S31

Fig. S1 Electronic absorption spectra of complexes **1** – **4** in CH_3CN at 298 K. S32

Fig. S2 Normalised emission spectra of complexes **1** – **4** in CH_3CN at 298 K (red) and alcohol glass at 77 K (blue). S33

Fig. S3 (a) Emission spectra of complex **2** (10 μM) in the absence (black) and presence (red) of BCN-OH (500 μM) in aerated PBS/DMSO (9:1, *v*/*v*) at 298 K for 16 h. (b) ESI-mass spectrum of the product from the reaction between complex **2** and BCN-OH in CH_3OH at 298 K. S34

Fig. S4 HPLC chromatograms of complex **1** (25 μM) (black) and a reaction mixture of complex **1** (25 μM) and c(RGDfC) (25 μM) (red) in ammonium acetate buffer (50 mM, pH 7.4)/DMF (9:1, *v*/*v*) containing TCEP (100 μM) after incubation at 37°C for 4 h. The absorbance was monitored at 210 nm. S35

Fig. S5 (a) HPLC chromatogram of the purified conjugate **1-RGD**. The absorbance was monitored at 350 nm. (b) ESI-mass spectrum of the purified conjugate **1-RGD** in CH_3CN at 298 K. S36

Fig. S6 (a) Emission spectra of conjugate **1-RGD** (10 μM) in the absence (black) or presence (red) of BCN-OH (500 μM) in aerated PBS/DMSO (9:1, *v*/*v*) at 298 K for 16 h. (b) ESI-mass spectrum of the product from the reaction between conjugate **1-RGD** and BCN-OH in CH_3OH at 298 K. S37

Fig. S7 Cellular uptake of conjugate **1-RGD** (20 μM, 1 h) in the presence of different inhibitors/conditions toward U87-MG cells. Control: incubation at 37°C; low-temperature: incubation at 4°C; cation transporter inhibitor: Et_4NCl (1 mM); metabolic inhibitors: 2-deoxy-D-glucose (50 mM) and oligomycin (5 μM); endocytic inhibitors: NH_4Cl (50 mM) or chloroquine (100 μM). The error bars correspond to the standard deviation of three replicates. S38

Fig. S8 LSCM images of live U87-MG, MCF-7 and HEK293 cells pretreated without (upper) or with (lower) RGD peptide (50 μM, 30 min), incubated with complex **2** (5 μM, 4 h; λ_{ex} = 405 nm, λ_{em} = 600 – 700 nm) and followed by continuous photoirradiation at 450 nm (10 mW cm^{-2}) for 20 min. Scale bar = 20 μm. S39

Fig. S9 Flow cytometric results of (a) U87-MG, (b) MCF-7 and (c) HEK293 cells incubated with blank medium for 4 h (orange) or conjugate **1-RGD** (5 μM, 4 h) before (blue) or after (red) photoirradiation at 450 nm (10 mW cm^{-2}) for 20 min. S40

Fig. S10 ESI-mass spectrum of the lysate of U87-MG cells incubated with conjugate **1-RGD** (5 μM, 4 h) followed by photoirradiation at 450 nm (10 mW cm^{-2}) for 20 min. S41

Fig. S11 LSCM images of live U87-MG, MCF-7 and HEK293 cells incubated S42

with complex **2** (5 μM, 4 h; λ_{ex} = 405 nm, λ_{em} = 600 – 700 nm) without (upper) or with (lower) photoirradiation at 450 nm (10 mW cm^{-2}) for 20 min. Scale bar = 20 μm.

Fig. S12 LSCM images of live U87-MG cells pretreated with conjugate **1-RGD** or complex **2** (5 μM, 4 h; λ_{ex} = 405 nm, λ_{em} = 600 – 700 nm) and then treated with BCN-OH (250 μM, 4 h) followed by incubation with MitoTracker Deep Red (100 nM, 20 min; λ_{ex} = 635 nm, λ_{em} = 650 – 680 nm). Scale bar = 20 μm. Pearson's correlation coefficient (PCC) = 0.96 (**1-RGD**) and 0.97 (**2**). S43

Fig. S13 LSCM images of live/dead cell staining of **1-RGD**-pretreated (5 μM, 4 h) U87-MG cells without (upper) or with (lower) continuous photoirradiation at 450 nm (10 mW cm^{-2}) for 20 min, followed by incubation with Calcein-AM (1 μM, 1 h; λ_{ex} = 488 nm, λ_{em} = 500 – 520 nm) and propidium iodide (10 μM, 1 h; λ_{ex} = 532 nm, λ_{em} = 600 – 650 nm). Scale bar = 20 μm. S44

Fig. S14 LSCM images of intracellular ROS of U87-MG cells pretreated with conjugate **1-RGD** (5 μM, 4 h) (a) without or (b) with photoirradiation at 450 nm (10 mW cm^{-2}) for 20 min and further incubation with CM-H_2DCFDA (5 μM, 30 min; λ_{ex} = 488 nm, λ_{em} = 500 – 550 nm). Scale bar = 20 μm. S45

Fig. S15 ^{1}H NMR spectrum of bpy-CONH-SH in DMSO-d_6 at 298 K. S46

Fig. S16 ^{1}H NMR spectrum of bpy-CONH-S-Tz-Cl in DMSO-d_6 at 298 K. S47

Fig. S17 ^{1}H NMR spectrum of bpy-CONH-S-Tz-S-Et in DMSO-d_6 at 298 K. S48

Fig. S18 ^{1}H NMR spectrum of bpy-CONH-SCN in DMSO-d_6 at 298 K. S49

Fig. S19	^{1}H NMR spectrum of bpy-$CONH_2$ in DMSO-d_6 at 298 K.	S50
Fig. S20	^{1}H NMR spectrum of complex **1** in DMSO-d_6 at 298 K.	S51
Fig. S21	^{13}C NMR spectrum of complex **1** in DMSO-d_6 at 298 K.	S52
Fig. S22	HR-ESI mass spectra of complex **1** in CH_3CN.	S53
Fig. S23	^{1}H NMR spectrum of complex **2** in DMSO-d_6 at 298 K.	S54
Fig. S24	^{13}C NMR spectrum of complex **2** in DMSO-d_6 at 298 K.	S55
Fig. S25	HR-ESI mass spectra of complex **2** in CH_3CN.	S56
Fig. S26	^{1}H NMR spectrum of complex **3** in DMSO-d_6 at 298 K.	S57
Fig. S27	^{13}C NMR spectrum of complex **3** in DMSO-d_6 at 298 K.	S58
Fig. S28	HR-ESI mass spectra of complex **3** in CH_3CN.	S59
Fig. S29	^{1}H NMR spectrum of complex **4** in DMSO-d_6 at 298 K.	S60
Fig. S30	^{13}C NMR spectrum of complex **4** in DMSO-d_6 at 298 K.	S61
Fig. S31	HR-ESI mass spectra of complex **4** in CH_3CN.	S62
References		S63

Experimental Section

Materials and Instrumentation

All solvents were of analytical grade and purified according to standard procedures.[1] 2-Aminoethanethiol hydrochloride, Na_2CO_3, NH_4Cl, $MgSO_4$, triethylamine (Et_3N) and KPF_6 were purchased from Acros. Potassium thiocyanate, 4,4'-dimethyl-2,2'-bipyridine, SeO_2, $Na_2S_2O_5$, ethanethiol, colchicine, 2-phenylquinoline-4-carboxylic acid, 1,3-diphenylisobenzofuran (DPBF), (1*R*,8*S*,9*s*)-bicyclo[6.1.0]non-4-yn-9-ylmethanol (BCN-OH) and 3-(4,5-dimethylthiazol-2-yl)-2,5-diphenyltetrazolium bromide (MTT) were purchased from Sigma-Aldrich. $IrCl_3 \cdot 3H_2O$ was sourced from Precious Metals Online. 2-Bromoethylamine hydrobromide was purchased from ABCR. 3,6-Dichloro-1,2,4,5-tetrazine, NaCl and carbonyldiimidazole (CDI) were purchased from Energy Chemical. The cyclic RGD peptide (c(RGDfC)) was obtained from GL Biochem. 2-Phenylquinoline-4-carboxylic acid methyl ester (Hpqe),[2] 4-carboxyl acid-4'-methyl-2,2'-bipyridine (bpy-COOH)[3] and the iridium(III) dimer $[Ir_2(pqe)_4Cl_2]$[4] were prepared as reported previously. All buffer components were of biological grade and used as received. Dulbecco's modified Eagle's Medium (DMEM), Minimum Essential Medium (MEM), fetal bovine serum (FBS), penicillin/streptomycin, trypsin-EDTA, phosphate-buffered saline (PBS) at pH 7.4, Alexa Fluor 647–Annexin V conjugate, propidium iodide, CM-H_2DCFDA, MitoTracker Deep Red, CellMask Deep Red and CellEvent Caspase-3/7 Red were purchased from Invitrogen. Calcein-AM, rhodamine 123 and Hoechst 33342 were ordered from Beyotime. Autoclaved Milli-Q water was used for the preparation of aqueous solutions. U87-MG, MCF-7 and HEK293 cells were obtained from American Type Culture Collection. The growth medium for cell culture contained DMEM or MEM with 10% FBS and 1% penicillin/streptomycin.

^1H and ^{13}C NMR spectra were recorded on a Bruker AVANCE III 300, 400 or 600 MHz

spectrometer at 298 K using deuterated solvents. Chemical shifts (δ, ppm) were reported relative to tetramethylsilane (TMS). Positive-ion electrospray ionisation mass spectra (ESI-MS) were recorded on a Perkin-Elmer Sciex API 3200MD mass spectrometer. High-resolution electrospray ionisation mass spectra (HR-ESI-MS) were recorded on a Bruker micrOTOF-QII. IR spectra of the samples in KBr pellets were recorded in the range of 4000 – 400 cm^{-1} using a Perkin Elmer FTIR–1600 spectrometer. High performance liquid chromatography (HPLC) was performed on an Agilent 1260 Infinity II system coupled with a diode array detector WR using H_2O containing 0.1% (*v*/*v*) trifluoroacetic acid (TFA) (solvent A) and CH_3CN containing 0.1% (*v*/*v*) TFA (solvent B) as the solvents and the detector was set at 350 nm. The HPLC purifications were performed on an Agilent semi-preparative column (ZORBAX Eclipse XDB-C18 column: 9.4 × 250 mm, 5 μm) with a linear gradient of 50 – 100% B over 20 min and a flow rate of 3 mL min^{-1}. The HPLC analyses were carried out using an Agilent analytical column (ZORBAX Eclipse Plus C18: 4.6 × 150 mm, 5 μm) with a linear gradient of 10 to 100% B and a flow rate of 1 mL min^{-1}.

Synthesis

4-(*N*-Mercaptoethylaminocarbonyl)-4'-methyl-2,2'-bipyridine (bpy-CONH-SH)

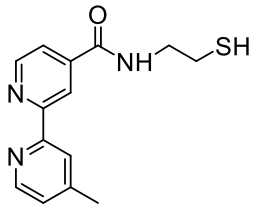

A mixture of bpy-COOH (100 mg, 0.47 mmol) and CDI (84.3 mg, 0.52 mmol) in dry DMF was stirred at room temperature under an inert atmosphere of nitrogen in the dark for 30 min. 2-Aminoethanethiol hydrochloride (53.4 mg, 0.47 mmol) was added and the mixture was further stirred at room temperature for 6 h. The solvent was removed under reduced pressure and the remaining white solid was purified by column chromatography on silica gel using CH_2Cl_2/CH_3OH (50:1, *v*/*v*) as the eluent. The solvent was removed under reduced pressure to afford the product as a white solid. Yield: 65 mg (51%). ^{1}H NMR (400 MHz, DMSO-d_6, 298 K, TMS): δ 9.01 (t, J = 5.4 Hz, 1H, NH of bpy-CONH-SH), 8.82 (d, J = 5.0 Hz, 1H, H6 of bpy), 8.77 (s, 1H, H3 of bpy), 8.59 (d, J = 5.0 Hz, 1H, H6' of bpy), 8.28 (s, 1H, H3' of bpy), 7.82 – 7.80 (m, 1H, H5 of bpy), 7.34 (d, J = 4.3 Hz, 1H, H5' of bpy), 3.49 – 3.44 (m, 2H, CH_2 of $NHCH_2CH_2$), 2.69 (t, J = 6.6 Hz, 2H, $NHCH_2CH_2$), 2.44 (s, 3H, CH_3 of bpy). ESI-MS (positive-ion mode): m/z 274 $[M + H^+]^+$.

4-(*S*-(6-Chloro-1,2,4,5-tetrazin-3-yl)-*N*-mercaptoethylaminocarbonyl)-4'-methyl-2,2'-bipyridine (bpy-CONH-S-Tz-Cl)

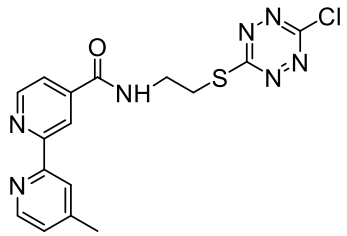

To a solution of 3,6-dichloro-1,2,4,5-tetrazine (84.5 mg, 0.56 mmol) in CH_2Cl_2 (20 mL), a mixture of bpy-CONH-SH (100 mg, 0.37 mmol) and Et_3N (77.7 μL, 0.56 mmol) in CH_2Cl_2 (20 mL) was slowly added. The resulting mixture was stirred at room temperature under an inert atmosphere of nitrogen in the dark for 6 h. The solvent was removed under reduced pressure and the crude red solid was purified by column chromatography on silica gel using CH_2Cl_2/CH_3OH (100:1, *v*/*v*) as the eluent. The solvent was removed under reduced pressure to afford the product as a red solid. Yield: 143.5 mg (51%). ^{1}H NMR (400 MHz, DMSO-d_6, 298 K, TMS): δ 9.27 (t, J = 5.5 Hz, 1H, NH of bpy-CONH-SH), 8.83 (d, J = 5.0 Hz, 1H, H6 of bpy), 8.75 (s, 1H, H3 of bpy), 8.59 (d, J = 5.0 Hz, 1H, H6' of bpy), 8.29 (s, 1H, H3' of bpy), 7.81 – 7.80 (m, 1H, H5 of bpy), 7.35 (d, J = 4.3 Hz, 1H, H5' of bpy), 3.76 – 3.71 (m, 2H, $NHCH_2CH_2$), 2.71 – 2.67 (m, 2H, $NHCH_2CH_2$), 2.45 (s, 1H, CH_3 of bpy). ESI-MS (positive-ion mode): *m*/*z* 388 $[M + H^+]^+$.

4-(*S*-(6-Ethylthio-1,2,4,5-tetrazin-3-yl)-*N*-mercaptoethylaminocarbonyl)-4'-methyl-2,2'-bipyridine (bpy-CONH-S-Tz-S-Et)

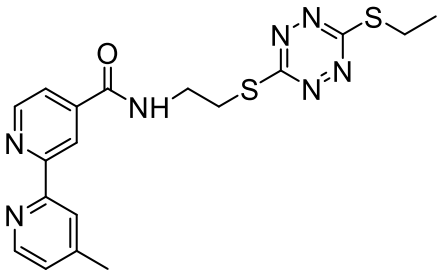

A mixture of bpy-CONH-S-Tz-Cl (77.6 mg, 0.20 mmol), ethanethiol (24.9 mg, 0.40 mmol) and Et_3N (111.3 μL, 0.80 mmol) in CH_2Cl_2 (30 mL) was stirred at room temperature under an inert atmosphere of nitrogen in the dark for 6 h. The solvent was removed under reduced pressure and the crude orange solid was purified by column chromatography on silica gel using CH_2Cl_2/CH_3OH (50:1, *v*/*v*) as the eluent. The solvent was removed under reduced pressure to afford the product as an orange solid. Yield: 62.0 mg (75%). ^{1}H NMR (300 MHz, $CDCl_3$, 298 K, TMS): δ 9.22 (t, J = 5.1 Hz, 1H, NH of bpy-CONH-SH), 8.81 (d, J = 5.0 Hz, 1H, H6 of bpy), 8.72 (s, 1H, H3 of bpy), 8.58 (d, J = 5.0 Hz, 1H, H6 of bpy), 8.27 (s, 1H, H3' of bpy), 7.78 – 7.77 (m, 1H, H5 of bpy), 7.34 (d, J = 4.8 Hz, 1H, H5' of bpy), 3.74 – 3.69 (m, 2H, $NHCH_2CH_2$), 3.57 – 3.54 (m, 2H, $NHCH_2CH_2$), 3.27 – 3.21 (m, 2H, CH_2CH_3), 2.44 (s, 3H, CH_3 of bpy), 1.33 (t, J = 7.3 Hz, 3H, CH_2CH_3). ESI-MS (positive-ion mode): *m*/*z* 414 $[M + H^+]^+$.

4-(*N*-(Thiocyanatoethyl)aminocarbonyl)-4'-methyl-2,2'-bipyridine (bpy-CONH-SCN)

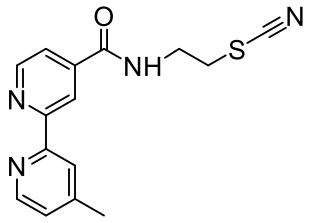

A mixture of 2-bromoethylamine hydrobromide (205 mg, 1.0 mmol) and potassium thiocyanate (292 mg, 3.0 mmol) in CH_3CN (20 mL) was stirred at room temperature under an inert atmosphere of nitrogen in the dark for 12 h. The solvent was removed under reduced pressure to yield a white solid. A mixture of bpy-COOH (107 mg, 0.5 mmol) and CDI (97 mg, 0.6 mmol) in dry DMF (10 mL) was stirred at room temperature under an inert atmosphere of nitrogen in the dark for 30 min. After that the white solid obtained from the last step in dry DMF (10 mL) was added and the resulting mixture was further stirred for 4 h. The solvent was removed under reduced pressure and the remaining white solid was purified by column chromatography on silica gel using CH_2Cl_2/CH_3OH (100:1, *v*/*v*) as the eluent. The solvent was removed under reduced pressure to afford the product as a white solid. Yield: 150 mg (80%). ^{1}H NMR (400 MHz, DMSO-d_6, 298 K, TMS): δ 9.80 (s, 1H, NH of bpy-CONH-SH), 9.90 (s, 1H, H3 of bpy), 8.81 (d, J = 6.6 Hz, 1H, H6 of bpy), 8.58 (d, J = 6.6 Hz, 1H, H6' of bpy), 8.27 (s, 1H, H3' of bpy), 7.94 – 7.92 (m, 1H, H5 of bpy), 7.32 (d, J = 5.4 Hz, 1H, H5' of bpy), 3.70 – 3.64 (m, 2H, $NHCH_2CH_2$), 3.34 – 3.28 (m, 2H, $NHCH_2CH_2$), 2.43 (s, 1H, CH_3 of bpy). ESI-MS (positive-ion mode): *m*/*z* 299 $[M + H^+]^+$.

4-Aminocarbonyl-4’-methyl-2,2’-bipyridine (bpy-$CONH_2$)

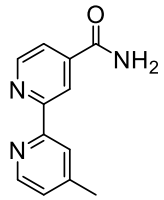

A mixture of bpy-COOH (250 mg, 1.2 mmol) and CDI (284.1 mg, 1.8 mmol) in dry DMF (10 mL) was stirred at 60°C under an inert atmosphere of nitrogen for 2 h. Then, a solution of NH_4Cl (84 mg, 1.6 mmol) and Et_3N (406 μL, 2.9 mmol) in dry DMF (10 mL) was added dropwise and stirring was continued at 60°C under an inert atmosphere of nitrogen for 16 h. The solvent was removed under reduced pressure and the residue was dissolved in CH_2Cl_2 (30 mL). The solution was filtered to remove unreacted bpy-COOH. The solvent was then removed under reduced pressure and the white crude product was purified by column chromatography on silica gel. The desired product was eluted using CH_2Cl_2/CH_3OH (30:1, *v*/*v*) as the eluent. The solvent was removed under reduced pressure to afford the product as a white solid. Yield: 186.6 mg (75%). ^{1}H NMR (400 MHz, DMSO-d_6, 298 K, TMS): δ 8.81 (d, J = 5.0 Hz, 1H, H6 of bpy), 8.78 (s, 1H, H3 of bpy), 8.58 (d, J = 4.9 Hz, 1H, H6’ of bpy), 8.40 (s, 1H, $CONH_2$), 8.27 (s, 1H, H3’ of bpy), 7.82 (dd, J_{gem} = 5.0 Hz, J_{vic} = 1.7 Hz, 1H, H5 of bpy), 7.76 (s, 1H, $CONH_2$), 7.33 (dd, J_{gem} = 4.9 Hz, J_{vic} = 0.8 Hz, 1H, H5’ of bpy), 3.70 – 3.64 (m, 2H, $NHCH_2CH_2$), 3.34 – 3.28 (m, 2H, $NHCH_2CH_2$), 2.43 (s, 1H, CH_3 of bpy). ESI-MS (positive-ion mode): *m*/*z* 214 $[M + H^+]^+$.

[Ir(pqe)$_2$(bpy-CONH-S-Tz-Cl)](PF$_6$) (**1**)

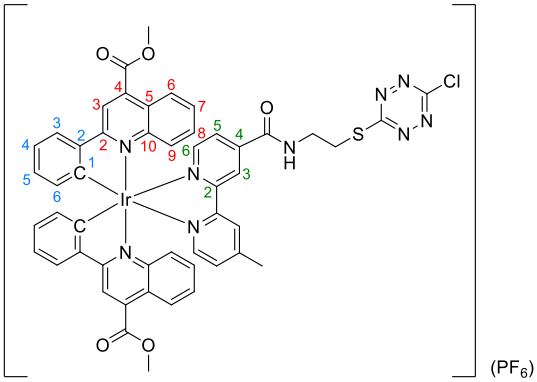

A mixture of [Ir$_2$(pqe)$_4$Cl$_2$] (60.2 mg, 0.04 mmol) and bpy-CONH-S-Tz-Cl (31.0 mg, 0.08 mmol) in CH_2Cl_2 (30 mL) was stirred under an inert atmosphere of nitrogen for 12 h. After KPF_6 (66.3 mg, 0.36 mmol) in CH_3OH (2 mL) was added, the mixture was stirred for 30 min and then evaporated to dryness under vacuum. The crude red solid was purified by column chromatography on silica gel using CH_2Cl_2/CH_3OH (100:1, *v*/*v*) as the eluent. The solvent was removed under reduced pressure to yield a red solid. Subsequent recrystallisation of the red solid from CH_2Cl_2/Et_2O afforded the complex as red crystals. Yield: 31.9 mg (32%). ^{1}H NMR (400 MHz, DMSO-d_6, 298 K, TMS): δ 9.24 (t, J = 5.3 Hz, 1H, NH of bpy-CONH-Tz-Cl), 8.85 (s, 2H, H3 and H3' of quinolinyl ring of pqe), 8.68 (s, 1H, H3 of bpy), 8.39 – 8.33 (m, 5H, H3', H6 and H6' of bpy and H5 and H5' of quinolinyl ring of pqe), 8.23 (d, J = 5.7 Hz, 1H, H5 of bpy), 7.98 – 7.94 (m, 2H, H3 and H3' of phenyl ring of pqe), 7.60 (d, J = 5.7 Hz, 1H, H5' of bpy), 7.53 (t, J = 7.5 Hz, 2H, H8 and H8' of quinolinyl ring of pqe), 7.36 (t, J = 9.5 Hz, 2H, H6 and H6' of quinolinyl ring of pqe), 7.24 – 7.16 (m, 4H, H7 and H7' of quinolinyl ring of pqe and H4 and H4' of phenyl ring of pqe), 6.90 – 6.86 (m, 2H, H5 and H5' of phenyl ring of pqe), 6.46 (t, J = 8.7 Hz, 2H, H6 and H6' of phenyl ring of pqe), 4.16 (s, 6H, $COOCH_3$), 3.58 (t, J = 6.0 Hz, 2H, $NHCH_2CH_2$), 3.46 – 3.40 (m, 2H, $NHCH_2CH_2$), 2.45 (s, 3H, CH_3 of bpy). ^{13}C NMR (150 MHz, DMSO-d_6, 298 K, TMS): δ 174.71 (1C, SC of tetrazine), 169.81 (1C, $COOCH_3$ of pqe), 169.65 (1C, $COOCH_3$ of pqe), 169.57 (1C, CONH of bpy), 166.12 (1C, C2

of quinolinyl ring of pqe), 165.31 (1C, C2’ of quinolinyl ring of pqe), 165.27 (1C, C2 of bpy), 162.83 (1C, C2’ of bpy), 155.62 (1C, C10 of quinolinyl ring of pqe), 154.03 (1C, C10’ of quinolinyl ring of pqe), 152.24 (1C, C4 of bpy), 150.91 (1C, CCl of tetrazine), 150.87 (1C, C4’ of bpy), 148.16 (1C, C5 of bpy), 147.30 (1C, C5' of bpy), 146.64 (1C, C2 of phenyl ring of pqe), 145.23 (1C, C2’ of phenyl ring of pqe), 145.12 (1C, C4 of quinolinyl ring of pqe), 143.7 (1C, C4’ of quinolinyl ring of pqe), 139.22 (1C, C1 of phenyl ring of pqe), 139.16 (1C, C1’ of phenyl ring of pqe), 134.05 (2C, C5 and C5’ of quinolinyl ring of pqe), 133.98 (2C, C6 and C6’ of phenyl ring of pqe), 131.51 (2C, C4 and C4’ of phenyl ring of pqe), 131.34 (2C, C5 and C5’ of phenyl ring of pqe), 129.63 (2C, C9 and C9’ of quinolinyl ring of pqe), 128.38 (1C, C6 of bpy), 128.29 (1C, C6’ of bpy), 128.19 (1C, C6 of quinolinyl ring of pqe), 128.13 (1C, C3 of phenyl ring of pqe), 126.60 (1C, C3’ of phenyl ring of pqe), 126.51 (1C, C6’ of quinolinyl ring of pqe), 125.54 (1C, C3 of bpy), 124.69 (1C, C7 of quinolinyl ring of pqe), 123.55 (1C, C7’ of quinolinyl ring of pqe), 123.49 (1C, C8 of quinolinyl ring of pqe), 123.16 (1C, C8’ of quinolinyl ring of pqe), 121.61 (1C, C3’ of bpy), 118.71 (1C, C3 of quinolinyl ring of pqe), 118.59 (1C, C3’ of quinolinyl ring of pqe), 69.80 (1C, NH*C*$H_2$$CH_2$ of bpy), 56.28 (1C, COO*C*H_3 of pqe), 53.44 (1C, COO*C*H_3 of pqe), 29.39 (1C, NHCH_2*C*H_2 of bpy), 20.75 (1C, CH_3 of bpy). IR (KBr) $\tilde{\nu}$/cm^{-1}: 845 (PF_6^-). HR-ESI-MS (positive-ion mode, *m*/*z*): $[M - PF_6^-]^+$ calcd for $IrC_{50}H_{38}N_9O_5SCl$ 1104.2034, found 1104.2108.

[Ir(pqe)$_2$(bpy-CONH-S-Tz-S-Et)](PF$_6$) (**2**)

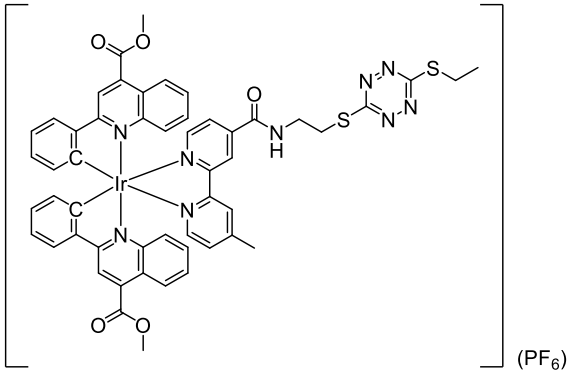

The synthetic procedure was similar to that of complex **1**, except that bpy-CONH-S-Tz-S-Et (49.6 mg, 0.08 mmol) was used instead of bpy-CONH-S-Tz-Cl. Subsequent recrystallisation of the red solid from CH_2Cl_2/Et_2O afforded the complex as red crystals. Yield: 71.4 mg (70%). ^{1}H NMR (400 MHz, DMSO-d_6, 298 K, TMS): δ 9.20 (t, J = 5.2 Hz, 1H, NH of bpy-CONH-TzCl), 8.86 (s, 2H, H3 and H3' of quinolinyl ring of pqe), 8.67 (s, 1H, H3 of bpy), 8.39 – 8.34 (m, 5H, H3', H6 and H6' of bpy and H5 and H5' of quinolinyl ring of pqe), 8.23 (d, J = 5.7 Hz, 1H, H5 of bpy), 7.97 – 7.95 (m, 2H, H3 and H3' of phenyl ring of pqe), 7.60 (d, J = 5.6 Hz, 1H, H5' of bpy), 7.53 (t, J = 7.6 Hz, 2H, H8 and H8' of quinolinyl ring of pqe), 7.36 (t, J = 9.1 Hz, 2H, H6 and H6' of quinolinyl ring of pqe), 7.24 – 7.16 (m, 4H, H7 and H7' of quinolinyl ring of pqe and H4 and H4' of phenyl ring of pqe), 6.91 – 6.86 (m, 2H, H5 and H5' of phenyl ring of pqe), 6.47 (t, J = 8.4 Hz, 2H, H6 and H6' of phenyl ring of pqe), 4.16 (s, 6H, $COOCH_3$), 3.68 – 3.63 (m, 2H, $NHCH_2CH_2$), 3.49 – 3.45 (m, 2H, $NHCH_2CH_2$), 3.25 – 3.20 (m, 2H, CH_2CH_3) 2.45 (s, 3H, CH_3 of bpy), 1.32 (t, J = 7.2 Hz, 3H, CH_2CH_3). ^{13}C NMR (150 MHz, DMSO-d_6, 298 K, TMS): δ 172.10 (1C, CH_2CH_2SC of tetrazine), 171.52 (1C, $CSCH_2CH_3$ of tetrazine), 169.68 (1C, $COOCH_3$ of pqe), 169.60 (1C, $COOCH_3$ of pqe), 165.32 (2C, C2 and C2' of quinolinyl ring of pqe), 163.14 (1C, CONH of bpy), 155.58 (2C, C2 and C2' of bpy), 153.82 (1C, C10 of quinolinyl ring of pqe), 152.23 (1C, C10' of quinolinyl ring of pqe), 150.90 (2C, C4 and C4' of bpy), 148.21 (1C, C5 of bpy), 147.34 (1C, C5' of bpy), 146.76 (1C, C2 of

phenyl ring of pqe), 145.24 (1C, C2’ of phenyl ring of pqe), 145.14 (1C, C4 of quinolinyl ring of pqe), 143.89 (1C, C4’ of quinolinyl ring of pqe), 139.25 (1C, C1 of phenyl ring of pqe), 139.20 (1C, C1’ of phenyl ring of pqe), 134.11 (2C, C5 and C5’ of quinolinyl ring of pqe), 134.01 (2C, C6 and C6’ of phenyl ring of pqe), 131.47 (2C, C4 and C4’ of phenyl ring of pqe), 131.31 (2C, C5 and C5’ of phenyl ring of pqe), 129.70 (2C, C9 and C9’ of quinolinyl ring of pqe), 128.40 (2C, C6 and C6’ of bpy), 128.15 (1C, C6 of quinolinyl ring of pqe), 126.55 (2C, C3 and C3’ of phenyl ring of pqe), 126.45 (1C, C6’ of quinolinyl ring of pqe), 125.34 (1C, C3 of bpy), 124.71 (1C, C7 of quinolinyl ring of pqe), 123.58 (1C, C7’ of quinolinyl ring of pqe), 123.32 (1C, C8 of quinolinyl ring of pqe), 123.21 (1C, C8’ of quinolinyl ring of pqe), 121.60 (1C, C3’ of bpy), 118.72 (1C, C3 of quinolinyl ring of pqe), 118.61 (1C, C3’ of quinolinyl ring of pqe), 53.47 (1C, COO*C*H_3 of pqe), 53.44 (1C, COO*C*H_3 of pqe), 29.07 (1C, NHCH_2*C*H_2 of bpy), 24.45 (1C, CH_3 of bpy). IR (KBr) $\tilde{\nu}$/cm^{-1}: 845 (PF_6^-). HR-ESI-MS (positive-ion mode, *m*/*z*): $[M - PF_6^-]^+$ calcd for $IrC_{52}H_{43}N_9O_5S_2$ 1130.2458, found 1130.2542.

[Ir(pqe)$_2$(bpy-CONH-SCN)](PF$_6$) (**3**)

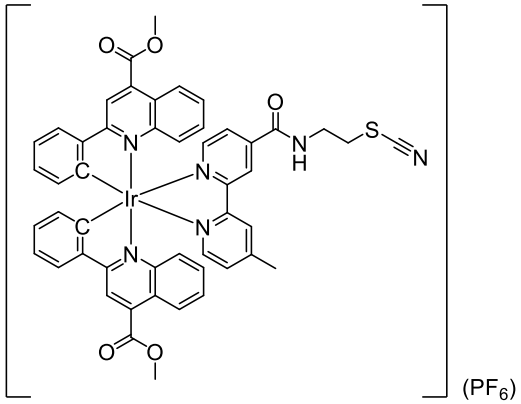

The synthetic procedure was similar to that of complex **1**, except that bpy-CONH-SCN (23.9 mg, 0.08 mmol) was used instead of bpy-CONH-S-Tz-Cl. Subsequent recrystallisation of the red solid from CH_2Cl_2/Et_2O afforded the complex as red crystals. Yield: 66.8 mg (72%). ^{1}H NMR (400 MHz, DMSO-d_6, 298 K, TMS): δ 8.85 (s, 1H, H3 of quinolinyl ring of pqe), 8.83 (s, 1H, H3' of quinolinyl ring of pqe), 8.72 (s, 1H, H3 of bpy), 8.46 (s, 1H, H3' of bpy), 8.38 – 8.31 (m, 4H, H6 and H6' of bpy and H5 and H5' of quinolinyl ring of pqe), 8.23 (d, J = 5.5 Hz, 1H, H5 of bpy), 8.07 (d, J = 5.2 Hz, 1H, H3 of phenyl ring of pqe), 7.92 (d, J = 5.5 Hz, 1H, H5' of bpy), 7.56 – 7.51 (m, 3H, H3' of phenyl ring of pqe and H8 and H8' of quinolinyl ring of pqe), 7.44 – 7.42 (m, 1H, H6 of quinolinyl ring of pqe), 7.35 – 7.33 (m, 1H, H6' of quinolinyl ring of pqe), 7.22 – 7.13 (m, 4H, H7 and H7' of quinolinyl ring of pqe and H4 and H4' of phenyl ring of pqe), 6.89 – 6.86 (m, 2H, H5 and H5' of phenyl ring of pqe), 6.46 (t, J = 8.6 Hz, 2H, H6 and H6' of phenyl ring of pqe), 4.16 (s, 6H, $COOCH_3$), 3.68 – 3.63 (m, 2H, $NHCH_2CH_2$), 3.49 – 3.45 (m, 2H, $NHCH_2CH_2$), 2.45 (s, 3H, CH_3 of bpy). ^{13}C NMR (150 MHz, DMSO-d_6, 298 K, TMS): δ 170.13 (1C, $COOCH_3$ of pqe), 170.03 (1C, $COOCH_3$ of pqe), 165.78 (1C, CONH of bpy), 165.73 (2C, C2 and C2' of quinolinyl ring of pqe), 156.05 (2C, C2 and C2' of bpy), 154.56 (1C, C10 of quinolinyl ring of pqe), 152.77 (1C, C10' of quinolinyl ring of pqe), 151.42 (1C, C4 of bpy), 148.72 (1C, C5 of bpy), 147.81 (1C, C4' of bpy), 147.66 (1C, C2 of phenyl ring of pqe), 147.00 (1C, C5' of bpy), 145.72 (1C, C2' of phenyl ring of pqe),

145.54 (2C, C4 and C4’ of quinolinyl ring of pqe), 139.68 (2C, C1 and C1’ of phenyl ring of pqe), 139.55 (2C, C5 and C5’ of quinolinyl ring of pqe), 134.47 (1C, C6 of phenyl ring of pqe), 134.41 (1C, C6’ of phenyl ring of pqe), 131.94 (2C, C4 and C4’ of phenyl ring of pqe), 131.71 (2C, C5 and C5’ of phenyl ring of pqe), 129.94 (2C, C9 and C9’ of quinolinyl ring of pqe), 128.84 (1C, C6 of bpy), 128.74, (1C, C6’ of bpy), 128.64 (1C, C6 of quinolinyl ring of pqe), 128.52 (1C, C3 of phenyl ring of pqe), 127.48 (1C, C3’ of phenyl ring of pqe), 126.95 (1C, C6’ of quinolinyl ring of pqe), 125.84 (1C, C3’ of bpy), 125.28 (1C, C7 of quinolinyl ring of pqe), 125.08 (1C, C7’ of quinolinyl ring of pqe), 123.93 (1C, SCN of bpy), 123.57 (2C, C8 and C8’ of quinolinyl ring of pqe), 122.91 (1C, C3 of bpy), 119.15 (1C, C3 of quinolinyl ring of pqe), 119.03 (1C, C3’ of quinolinyl ring of pqe), 53.90 (1C, COO*C*H_3 of pqe), 53.85 (1C, COO*C*H_3 of pqe), 29.86 (1C, NHCH_2*C*H_2 of bpy), 21.11 (1C, CH_3 of bpy). IR (KBr) $\tilde{\nu}$/cm^{-1}: 845 (PF_6^-). HR-ESI-MS (positive-ion mode, *m*/*z*): $[M - PF_6^-]^+$ calcd for $IrC_{49}H_{38}N_6O_5S$ 1015.2254, found 1015.2343.

[Ir(pqe)$_2$(bpy-CONH$_2$)](PF$_6$) (**4**)

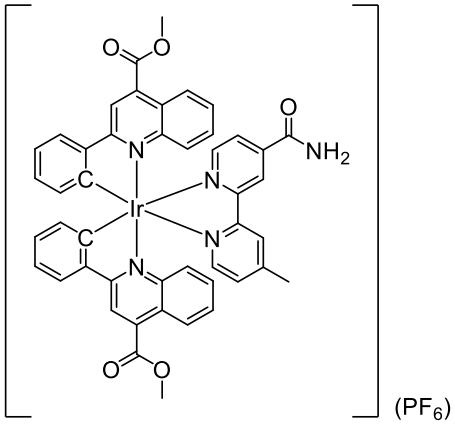

The synthetic procedure was similar to that of complex **1**, except that bpy-CONH$_2$ (17.1 mg, 0.08 mmol) was used instead of bpy-CONH-S-Tz-Cl. Subsequent recrystallisation of the red solid from CH_2Cl_2/Et_2O afforded the complex as red crystals. Yield: 60.1 mg (70%). ^{1}H NMR (400 MHz, DMSO-d_6, 298 K, TMS): δ 8.84 (s, 2H, H3 and H3' of quinolinyl ring of pqe), 8.71 (s, 1H, H3 of bpy), 8.42 (s, 1H, H3' of bpy), 8.38 – 8.33 (m, 5H, CONH$_2$, H6 and H6' of bpy and H5 and H5' of quinolinyl ring of pqe), 8.21 (d, J = 5.6 Hz, 1H, H5 of bpy), 8.04 (s, 1H, CONH$_2$), 7.98 – 7.93 (m, 2H, H3 and H3' of phenyl ring of pqe), 7.58 (d, J = 5.7 Hz, 1H, H5' of bpy), 7.54 – 7.50 (m, 2H, H8 and H8' of quinolinyl ring of pqe), 7.38 – 7.33 (m, 2H, H6 and H6'of quinolinyl ring of pqe), 7.23 – 7.16 (m, 4H, H7 and H7' of quinolinyl ring of pqe and H4 and H4' of phenyl ring of pqe), 6.90 – 6.87 (m, 2H, H5 and H5' of phenyl ring of pqe), 6.46 (t, J = 7.7 Hz, 2H, H6 and H6' of phenyl ring of pqe), 4.07 (s, 6H, COOCH$_3$), 2.50 (s, 3H, CH$_3$ of bpy). ^{13}C NMR (150 MHz, DMSO-d_6, 298 K, TMS): δ 170.10 (1C, *C*OOCH$_3$ of pqe), 170.03 (1C, *C*OOCH$_3$ of pqe), 165.76 (1C, CONH$_2$ of bpy), 165.74 (1C, C2 of quinolinyl ring of pqe), 164.81 (1C, C2' of quinolinyl ring of pqe), 156.02 (1C, C2 of bpy), 154.41 (1C, C2' of bpy), 152.66 (1C, C10 of quinolinyl ring of pqe), 151.39 (1C, C10' of quinolinyl ring of pqe), 151.28 (1C, C4 of bpy), 148.57 (1C, C5 of bpy), 147.75 (1C, C4' of bpy), 147.74 (1C, C2 of phenyl ring of pqe), 147.12 (1C, C5' of bpy), 145.68 (1C, C2' of phenyl ring of pqe), 145.57 (1C, C4 of quinolinyl ring of pqe), 144.61 (1C, C4' of quinolinyl ring of pqe), 139.66 (2C, C1 and C1'

of phenyl ring of pqe), 139.61 (2C, C5 and C5’ of quinolinyl ring of pqe), 134.55 (1C, C6 of phenyl ring of pqe), 134.46 (1C, C6’ of phenyl ring of pqe), 131.92 (2C, C4 and C4’ of phenyl ring of pqe), 131.80 (2C, C5 and C5’ of phenyl ring of pqe), 131.74 (2C, C9 and C9’ of quinolinyl ring of pqe), 130.08 (1C, C6 of bpy), 128.83 (1C, C6’ of bpy), 128.75 (1C, C6 of quinolinyl ring of pqe), 128.63 (1C, C3 of phenyl ring of pqe), 126.98 (1C, C3’ of phenyl ring of pqe), 125.84 (1C, C6’ of quinolinyl ring of pqe), 125.15 (1C, C3’ of bpy), 124.00 (1C, C7 of quinolinyl ring of pqe), 123.94 (1C, C7’ of quinolinyl ring of pqe), 123.62 (2C, C8 and C8’ of quinolinyl ring of pqe), 122.18 (1C, C3 of bpy), 119.16 (1C, C3 of quinolinyl ring of pqe), 119.04 (1C, C3’ of quinolinyl ring of pqe), 53.90 (1C, COO*C*H_3 of pqe), 53.87 (1C, COO*C*H_3 of pqe), 21.24 (1C, CH_3 of bpy). IR (KBr) $\tilde{\nu}$/cm^{-1}: 845 (PF_6^-). HR-ESI-MS (positive-ion mode, *m*/*z*): $[M - PF_6^-]^+$ calcd for $IrC_{49}H_{38}N_6O_5S$ 930.2267, found 930.2266.

Preparation of Conjugate 1-RGD

A mixture of complex **1** (2.0 μmol) and c(RGDfC) peptide (2.0 μmol) in acetate buffer (50 mM, pH 6.0)/DMF (9:1, *v*/*v*, 1 mL) containing TCEP (12 μmol) was stirred at 37°C in the dark for 12 h. The solvent was removed under reduced pressure and the residual solid was dissolved with a mixture of H_2O and CH_3CN (4 mL, *v*/*v*, 1:1) and purified in batches by semi-preparative RP-HPLC. The HPLC purifications were performed on an Agilent semi-preparative column (ZORBAX Eclipse XDB-C18 column: 9.4 × 250 mm, 5 μm) using H_2O containing 0.1% (*v*/*v*) TFA (solvent A) and CH_3CN containing 0.1% (*v*/*v*) TFA (solvent B) as the solvents with a linear gradient of 50 – 100% B over 20 min and a flow rate of 3 mL min^{-1}. The detector was set at 210 nm and fractions containing the product were combined and lyophilised. The HPLC analyses were carried out using an Agilent analytical column (ZORBAX Eclipse Plus C18: 4.6 × 150 mm, 5 μm) with a linear gradient of 30 – 100% B over 25 min and a flow rate of 1 mL min^{-1}. **1-RGD**. Yield: 2.6 mg (75%). Positive-ion ESI-MS ion clusters at *m*/*z* 824.3 $[M - CF_3CO_2^- + H^+]^{2+}$.

Photophysical Measurements

Electronic absorption spectra were recorded on an Agilent 8453 diode array spectrophotometer. Steady-state emission spectra were recorded on a HORIBA FluoroMax-4 spectrofluorometer. Unless specified otherwise, all solutions for photophysical studies were degassed with no fewer than four successive freeze-pump-thaw cycles and stored in a 10-cm^3 round bottomed flask equipped with a side-arm 1-cm fluorescence cuvette and sealed from the atmosphere by a Rotaflo HP6/6 quick-release Teflon stopper. Emission quantum yields (Φ_{em}) were measured by the optically dilute method using an aerated aqueous solution of the $[Ru(bpy)_3]Cl_2$ ($\Phi_{em} = 0.040$, λ_{ex} = 455 nm) as the standard solution.[5] The concentrations of the standard and sample solutions were adjusted until the absorbance at 455 nm was 0.1. Emission lifetimes were measured on an Edinburgh Instruments LP920 laser flash photolysis spectrometer using the third harmonic output (375 nm; 6 – 8 ns fwhm pulse width) of a Spectra-Physics Quanta-Ray Q-switched LAB-150 pulsed Nd:YAG laser (10 Hz) as the excitation source.

Determination of Singlet Oxygen ($^1O_2$) Generation Quantum Yield (Φ_Δ)

The $^1O_2$ generation quantum yields were determined by detecting the oxidation of DPBF using absorbance measurements.[6] An aerated CH_3CN solution (2 mL) containing the iridium(III) complexes or conjugate and DPBF (100 μM) was introduced to a 1-cm path length quartz cuvette and photoirradiated at 450 nm using a Xenon lamp (Ushio) (150 W) with a bandwidth of 20 nm. $[Ru(bpy)_3]Cl_2$ was used as a reference for $^1O_2$ sensitisation (Φ_Δ = 0.57 in aerated CH_3CN).[7] The absorbance of DPBF at *ca.* 418 nm would decrease upon the irreversible 1,4-cycloaddition reaction of DPBF induced by $^1O_2$. The following equation was used for the calculation of Φ_Δ:

$$\Phi_\Delta^{unknown} = \Phi_\Delta^{reference} \times \frac{m^{unknown} \times F^{reference}}{m^{reference} \times F^{unknown}}$$

where m is the slope of a linear fit of the change of absorbance at 418 nm against the irradiation time and F is the absorption correction factor, which is given as $F = 1 - 10^{-AL}$ (A = absorbance at 450 nm and L = path length of the cuvette).

Cell Cultures

U87-MG cells were cultured in MEM containing 10% FBS and 1% penicillin/streptomycin in an incubator at 37°C under a 5% CO_2 atmosphere. MCF-7 and HEK293 cells were cultured in DMEM containing 10% FBS and 1% penicillin/streptomycin in an incubator at 37°C under a 5% CO_2 atmosphere. Cells were passaged by dissociation from the adherent state with 0.25% trypsin in PBS (pH 7.4) to retain their viability when 70 – 80% confluence was reached.

ICP-MS Measurements

U87-MG, MCF-7 or HEK293 cells were grown in a 35-mm tissue culture dish and incubated at 37°C under a 5% CO_2 atmosphere for 48 h. The culture medium was removed and replaced with a fresh medium containing conjugate **1-RGD** or complexes **2** – **4** (5 μM, 4 h) at 37°C under a 5% CO_2 atmosphere and the cells were washed with PBS (1 mL × 3). The cells were then trypsinised and harvested with PBS (1 mL). The cell number was counted with a Logos Biosystems LUNA-II automated cell counter. The harvested cells were digested with 65% HNO_3 (1 mL) at 60°C for 2 h, allowed to cool to room temperature and analysed by a NexION 2000 ICP-MS instrument (PerkinElmer SCIEX Instruments).

For experiments investigating the integrin-mediated cellular uptake, U87-MG cells were pretreated with free RGD peptide (50 μM, 30 min) at 37°C under a 5% CO_2 atmosphere and the cells were washed with PBS (1 mL × 3). The cells were then treated with conjugate **1-RGD** or complex **2** (5 μM, 4 h) at 37°C under a 5% CO_2 atmosphere and the cells were washed with

PBS (1 mL × 3). The cells were then trypsinised, harvested with PBS and digested with 65% HNO_3 for ICP-MS analysis.

Live-cell Confocal Imaging

U87-MG, MCF-7 or HEK293 cells in growth medium were seeded on a sterilised coverslip in a 35-mm tissue culture dish and grown at 37°C under a 5% CO_2 atmosphere for 48 h. In the photoactivation experiments, the cells were first treated with conjugate **1-RGD** or complex **2** (5 μM, 4 h) in growth medium at 37°C under a 5% CO_2 atmosphere, followed by photoirradiation at 450 nm (10 mW cm^{-2}) for 20 min using a cellular photocytotoxicity irradiator (PURI Materials, Shenzhen, China), washed with PBS (1 mL × 3) and then imaged using a Leica TCS SPE (inverted configuration) confocal microscope with an oil immersion 63× oil-immersion objective lens. In the experiments examining the phosphorogenic response towards BCN-OH, the cells were first treated with conjugate **1-RGD** or complex **2** (5 μM, 4 h), washed with PBS (1 mL × 3), then incubated with BCN-OH (250 μM, 4 h) in growth medium at 37°C under a 5% CO_2 atmosphere, washed with PBS (1 mL × 3) and then were imaged. In the experiments examining the phosphorogenic response towards photoirradiation, after incubation with conjugate **1-RGD** or complex **2** (5 μM, 4 h), the cells were washed with PBS (1 mL × 3), photoirradiation at 450 nm (10 mW cm^{-2}) for 20 min and then imaged using a Leica TCS SPE. In the co-staining experiments, the treated cells were further incubated with MitoTracker Deep Red (100 nM, 20 min; λ_{ex} = 635 nm) in growth medium at 37°C under a 5% CO_2 atmosphere, washed with PBS (1 mL × 3) and then imaged using a Leica TCS SPE. For co-staining experiments of complexes **3** and **4**, the conditions were the same as conjugate **1-RGD** and complex **2**, except that the samples were not photoirradiated. The PCCs were determined using the program ImageJ (Version 1.4.3.67).

Cellular Uptake Mechanism Studies

U87-MG cells in growth medium were seeded on a sterilised coverslip in a 35-mm tissue culture dish and grown at 37°C under a 5% CO_2 atmosphere for 48 h. The uptake mechanism was investigated by pretreatment of the cells with various pathway inhibitors and measurement of the iridium content inside the cells using a NexION 2000 ICP-MS instrument (PerkinElmer SCIEX Instruments). In the control experiments, the cells were incubated with conjugate **1-RGD** (20 μM) in DMEM/DMSO (99:1, *v*/*v*) at 37°C under a 5% CO_2 atmosphere for 1 h. In the low-temperature experiments, the cells were preincubated at 4°C for 1 h; in the metabolic inhibition experiments, the cells were pretreated with 2-deoxy-D-glucose (50 mM) and oligomycin (5 μM) for 1 h; in the endocytic inhibition experiments, the cells were pretreated with ammonium chloride (50 mM) or chloroquine (100 μM) for 1 h; in the cation transporter inhibition experiments, the cells were pretreated with Et_4NCl (1 mM) for 1 h. After the pretreatment, the cells were washed with PBS (1 mL × 3) and then treated with conjugate **1-RGD** (20 μM) in DMEM/DMSO (99:1, *v*/*v*) at 37°C under a 5% CO_2 atmosphere for 1 h. The medium containing the conjugate was removed and the cell layer was subsequently washed with PBS (1 mL × 3). Then, the cells were trypsinised and harvested with PBS (1 mL). The resultant mixture was treated with 65% HNO_3 (1 mL) at 70°C for 2 h, allowed to cool to room temperature and analysed.

Analysis of Cell Lysate of U87-MG Cells Treated with Conjugate 1-RGD by ESI-MS

U87-MG cells in growth medium were seeded in a 6-well plate and grown at 37°C under a 5% CO_2 atmosphere for 48 h. The growth medium was replaced with conjugate **1-RGD** (5 μM) in medium and the cells were incubated at 37°C under a 5% CO_2 atmosphere for 4 h. The cells were then photoirradiated at 450 nm (10 mW cm^{-2}) or kept in the dark for 20 min. The cells were trypsinised and harvested with PBS (1 mL × 3) and lysed by probe sonication with 90

cycles of 10 seconds on, 10 seconds off, at 80 % power on an ice bath. The solvent of the resulting mixture was removed and CH_3OH was added. The mixture was then centrifuged at 10,000 rpm at 4°C and the supernatant was collected for ESI-MS analysis.

Live/Dead Cell Staining Assay

U87-MG cells in growth medium were seeded on sterilised coverslips in 35-mm tissue culture dishes and grown at 37°C under a 5% CO_2 atmosphere for 48 h. The growth medium was replaced with conjugate **1-RGD** (5 μM) in fresh medium and the cells were incubated at 37°C under a 5% CO_2 atmosphere for 4 h incubation. The cells then were photoirradiated at 450 nm (10 mW cm^{-2}) or kept in the dark for 20 min, followed by staining with Calcein-AM (1 μM; λ_{ex} = 488 nm, λ_{em} = 500 – 520 nm) and propidium iodide (10 μM; λ_{ex} = 543 nm, λ_{em} = 600 – 650 nm) in MEM/DMSO (99:1, *v*/*v*) for 1 h. The cells were then washed with PBS (1 mL × 3) and imaged using a Leica TCS SPE confocal microscope with an oil immersion 63× objective.

MTT Assays

U87-MG, MCF-7 or HEK293 cells were seeded in a 96-well flat-bottomed microplate (*ca.* 10,000 cells per well) in a growth medium (100 μL) and incubated at 37°C under a 5% CO_2 atmosphere for 48 h. The growth medium was removed and replaced with conjugate **1-RGD** or complexes **2** – **4** in growth medium/DMSO (99:1, *v*/*v*) at 37°C under a 5% CO_2 atmosphere for 4 h. After treatment, the medium was removed and replenished with phenol red-free growth medium (100 μL). One of the microplates was kept in the dark for 20 min, while the other microplate was photoirradiated at 450 nm (10 mW cm^{-2}) for 20 min. The growth medium was replaced with fresh medium (100 μL) and the cells were further incubated at 37°C under a 5% CO_2 atmosphere for 16 h. After replenishing the cells with fresh medium (90 μL) and a solution of MTT in PBS (10 μL, 5 mg mL^{-1}), the cells were incubated at 37°C under a 5% CO_2

atmosphere for 4 h. The growth medium was removed and DMSO (100 μL) was added to each well. The microplates were further incubated at 37°C under a 5% CO_2 atmosphere for 15 min. The absorbance of the solutions at 570 nm was measured with a SPECTRAmax 340 microplate reader (Molecular Devices Corp., Sunnyvale, CA).

Studies of the Cell Death Mechanism

The intracellular ROS levels were assessed by using a fluorogenic probe CM-H_2DCFDA,[8] The cytoplasmic membrane was stained by CellMask Deep Red.[9] The nucleus morphology was visualised by staining with Hoechst 33342.[10] Mitochondrial membrane potential was analysed using rhodamine 123 as the indicator.[11] Caspase 3/7 activity was monitored using CellEvent Caspase-3/7 Red.[12] U87-MG cells in growth medium were seeded on a sterilised coverslip in 35-mm tissue culture dishes and grown at 37°C under a 5% CO_2 atmosphere for 48 h. The culture medium was removed and replaced with conjugate **1-RGD** (5 μM, 4 h) in MEM/DMSO (99:1, *v*/*v*) at 37°C under a 5% CO_2 atmosphere. The cells were washed with PBS (1 mL × 3) and replenished with phenol red-free medium. The tissue culture dish was kept in the dark for 20 min or photoirradiated at 450 nm (10 mW cm^{-2}) for 20 min. The cells were washed with PBS (1 mL × 3) and subsequently stained with CM-H_2DCFDA (10 μM, 30 min; λ_{ex} = 488 nm, λ_{em} = 500 – 550 nm), CellMask Deep Red (5 μM, 15 min; λ_{ex} = 635 nm, λ_{em} = 650 – 700 nm), Hoechst 33342 (5 μM, 15 min; λ_{ex} = 405 nm, λ_{em} = 415 – 495 nm), rhodamine 123 (5 μM, 15 min; λ_{ex} = 488 nm, λ_{em} = 500 − 550 nm) or CellEvent Caspase-3/7 Red (20 μL, 1:100, 1 h; λ_{ex} = 590 nm, λ_{em} = 610 – 630 nm) in DMEM at 37°C under a 5% CO_2 atmosphere. The cells were washed with PBS (1 mL × 3) and then mounted onto a sterilised glass slide for imaging.

Annexin V/Propidium Iodide Assays

U87-MG cells in growth medium were seeded on two 6-well plates and grown at 37°C under a 5% CO_2 atmosphere for 48 h. U87-MG cells were treated with conjugate **1-RGD** (1 μM, 4 h) in MEM/DMSO (99:1, *v*/*v*) at 37°C under a 5% CO_2 atmosphere. The cells were washed with PBS (1 mL × 3) and fresh phenol red-free medium (100 μL) was added. The cells were photoirradiated at 450 nm (10 mW cm^{-2}) or kept in the dark for 20 min. After further incubation in fresh MEM (100 μL) at 37°C under a 5% CO_2 atmosphere for 1 h, the medium was removed, followed by washing with PBS (1 mL × 3). The cells were then trypsinised and centrifuged at 1500 rpm for 1 min and the resulting cell pellet was washed with PBS (1 mL) and subjected to centrifugation. The cells were resuspended in an Annexin V binding buffer (100 μL) in the flow cytometer tubes, followed by the addition of propidium iodide (2 μL, 100 μg mL^{-1}, 15 min; λ_{ex} = 561 nm) and Alexa Fluor 647–Annexin V conjugate (5 μL, 50 μL mL^{-1}, 15 min; λ_{ex} = 638 nm). The cell suspension was kept in the dark for 15 min, followed by the addition of Annexin V binding buffer (400 μL) and analysis by flow cytometer (Beckman CytoFLEX). The cells without any treatment were used as a control group for background correction. Cells treated with cisplatin (20 μM, 24 h) in MEM/saline (0.9% NaCl) (99:1, *v*/*v*) were used as positive controls. The experiments were performed in triplicates and analysed using the FlowJo V10 software.

Table S1 Electronic absorption spectral data of complexes **1** – **4** in CH_3CN at 298 K.

Complex	λ_{abs}/nm (ε/dm^3 mol^{-1} cm^{-1})
1	265 (71,715), 288 (54,905), 318 sh (25,275), SSSS (28,410), 371 sh (25,380), 460 (5,330)
2	271 sh (66,335), 287 (74,650), 318 sh (26,010), 355 (28,250), 370 sh (25,730), 457 (5,565)
3	265 (64,270), 290 (68,610), 351 (33,505), 368 sh (31,050), 457 (5,935)
4	263 (64,630), 290 (61,025), 318 sh (30,685), 355 (34,260), 368 sh (31,545), 459 (6,385)

sh: shoulder

Table S2 Singlet oxygen ($^1O_2$) quantum yields (Φ_Δ) of complexes **1** – **4** and conjugate **1-RGD** in aerated CH_3CN at 298 K (λ_{ex} = 450 nm).

Complex/Conjugate	Φ_Δ[a]
1	0.55
2	0.60
3	0.81
4	0.79
1-RGD	0.54

[a] DPBF was used as the $^1O_2$ scavenger and $[Ru(bpy)_3]Cl_2$ was adopted as the reference (Φ_Δ = 0.57 in aerated CH_3CN).[6]

Table S3 Cellular uptake of conjugate **1-RGD** and complexes **2** – **4** in U87-MG, MCF-7 and HEK293 cells without or with pretreatment of RGD peptide (50 μM, 30 min).

		Amount of iridium[a]/fmol		
Complex/Conjugate	Condition	U87-MG	MCF-7	HEK293
1-RGD	– RGD	0.70 ± 0.01	0.32 ± 0.02	0.032 ± 0.002
	+ RGD	0.34 ± 0.01	0.25 ± 0.01	0.030 ± 0.001
2	– RGD	1.2 ± 0.1	1.1 ± 0.1	0.25 ± 0.02
	+ RGD	1.3 ± 0.1	1.2 ± 0.1	0.22 ± 0.01
3	– RGD	2.1 ± 0.1	2.5 ± 0.1	0.77 ± 0.02
	+ RGD	2.2 ± 0.1	2.4 ± 0.2	0.74 ± 0.02
4	– RGD	1.1 ± 0.1	1.1 ± 0.1	0.38 ± 0.01
	+ RGD	1.1 ± 0.1	1.1 ± 0.1	0.38 ± 0.02

[a] Amount of iridium associated with an average cell upon incubation with conjugate **1-RGD** or complexes **2** – **4** (5 μM, 4 h) at 37°C as determined by ICP-MS.

Fig. S1 Electronic absorption spectra of complexes **1** – **4** in CH_3CN at 298 K.

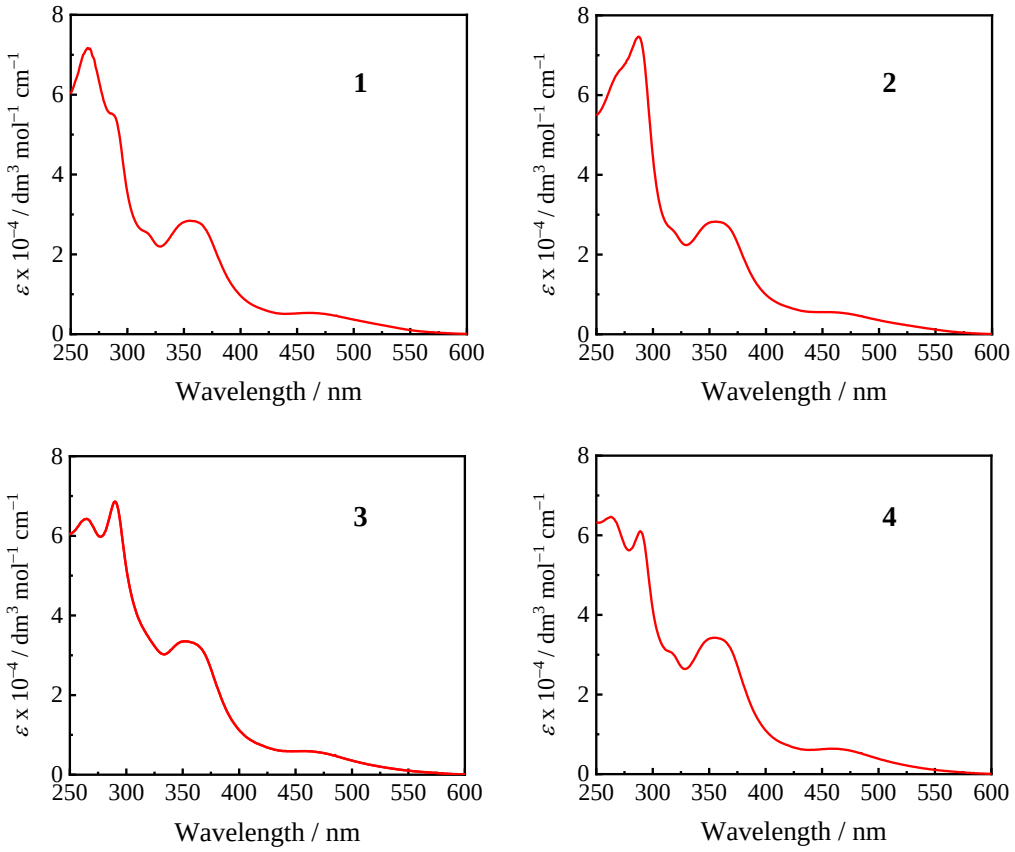

Fig. S2 Normalised emission spectra of complexes **1** – **4** in CH_3CN at 298 K (red) and alcohol glass at 77 K (blue).

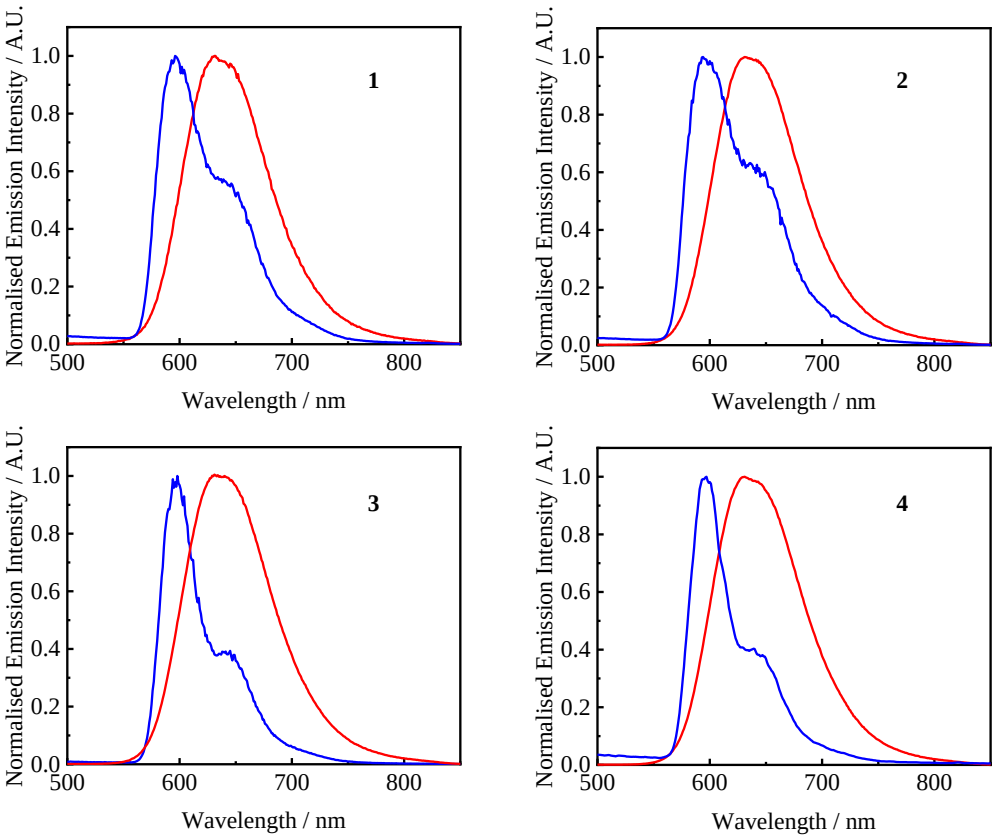

Fig. S3 (a) Emission spectra of complex **2** (10 μM) in the absence (black) and presence (red) of BCN-OH (500 μM) in aerated PBS/DMSO (9:1, *v*/*v*) at 298 K for 16 h. (b) ESI-mass spectrum of the product from the reaction between complex **2** and BCN-OH in CH_3OH at 298 K.

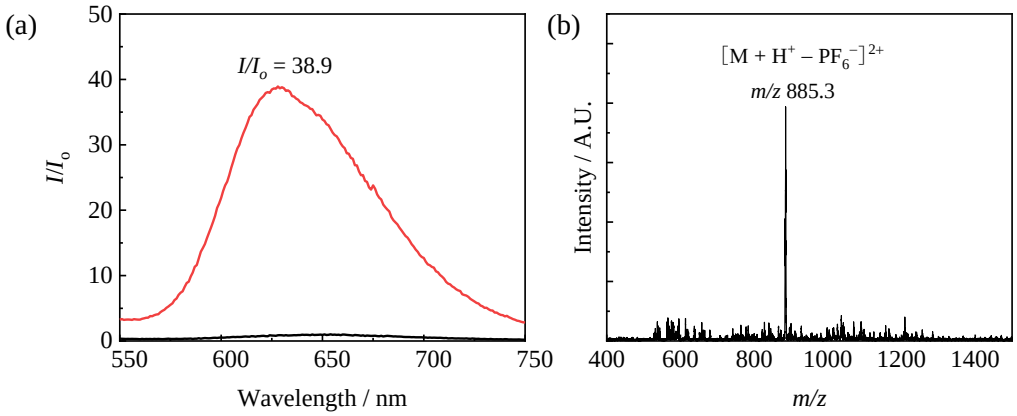

Fig. S4 HPLC chromatograms of complex **1** (25 μM) (black) and a reaction mixture of complex **1** (25 μM) and c(RGDfC) (25 μM) (red) in ammonium acetate buffer (50 mM, pH 7.4)/DMF (9:1, *v*/*v*) containing TCEP (100 μM) after incubation at 37°C for 4 h. The absorbance was monitored at 210 nm.

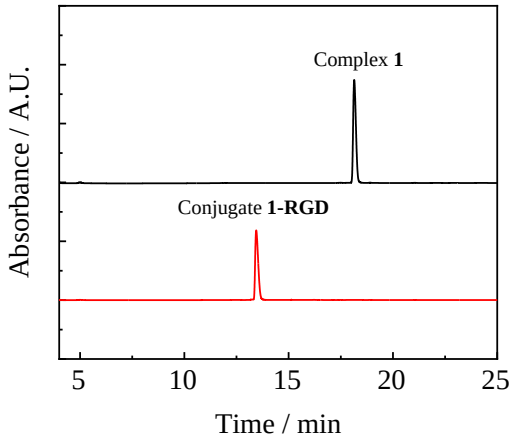

Fig. S5 (a) HPLC chromatogram of the purified conjugate **1-RGD**. The absorbance was monitored at 350 nm. (b) ESI-mass spectrum of the purified conjugate **1-RGD** in CH_3CN at 298 K.

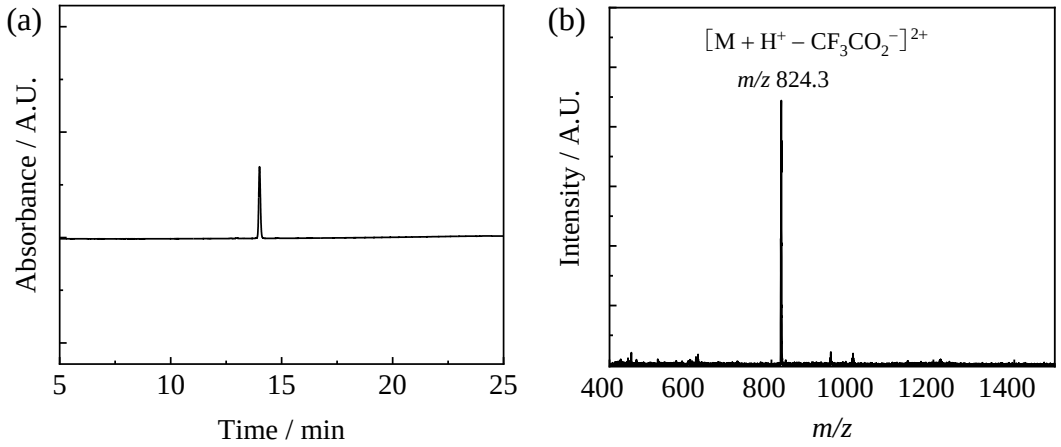

Fig. S6 (a) Emission spectra of conjugate **1-RGD** (10 μM) in the absence (black) or presence (red) of BCN-OH (500 μM) in aerated PBS/DMSO (9:1, *v*/*v*) at 298 K for 16 h. (b) ESI-mass spectrum of the product from the reaction between conjugate **1-RGD** and BCN-OH in CH_3OH at 298 K.

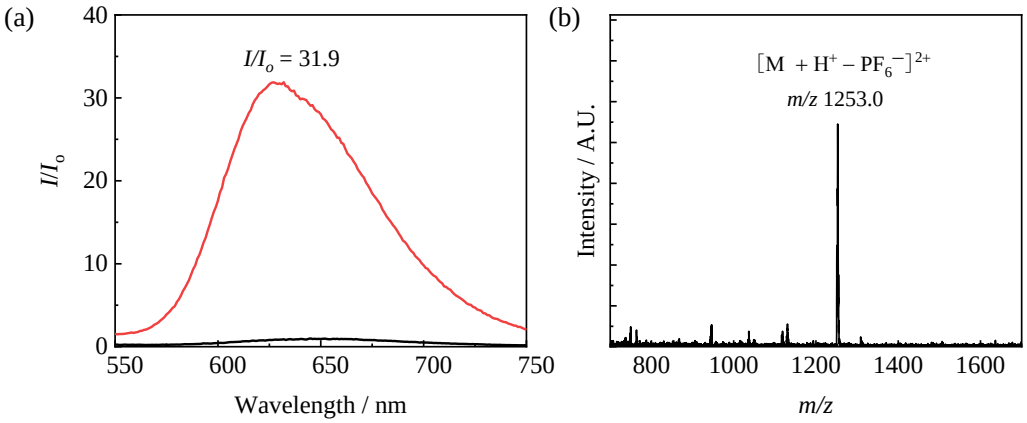

Fig. S7 Cellular uptake mechanism of conjugate **1-RGD** (20 μM, 1 h) in the presence of different inhibitors/conditions toward U87-MG cells. Control: incubation at 37°C; low-temperature: incubation at 4°C; cation transporter inhibitor: Et_4NCl (1 mM); metabolic inhibitors: 2-deoxy-D-glucose (50 mM) and oligomycin (5 μM); endocytic inhibitors: NH_4Cl (50 mM) or chloroquine (100 μM). The error bars correspond to the standard deviation of three replicates.

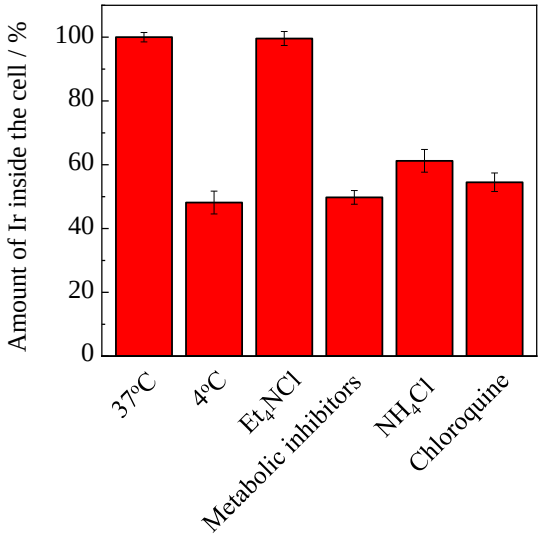

Fig. S8 LSCM images of live U87-MG, MCF-7 and HEK293 cells pretreated without (upper) or with (lower) RGD peptide (50 μM, 30 min), incubated with complex **2** (5 μM, 4 h; λ_{ex} = 405 nm, λ_{em} = 600 – 700 nm) and followed by continuous photoirradiation at 450 nm (10 mW cm^{-2}) for 20 min. Scale bar = 20 μm.

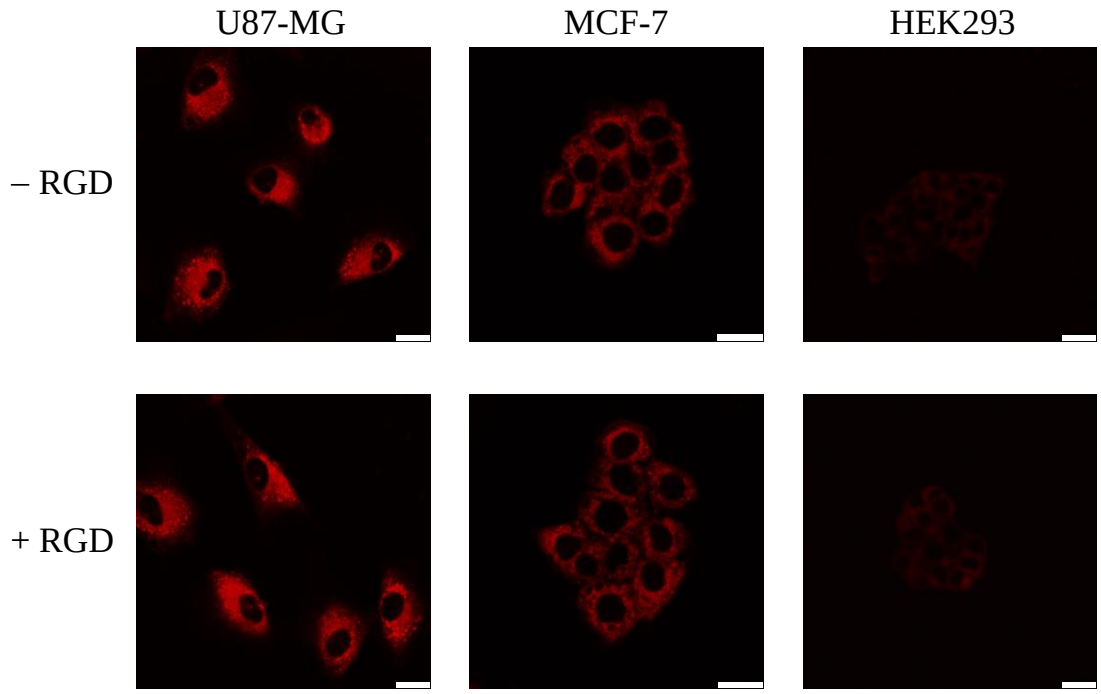

Fig. S9 Flow cytometric results of (a) U87-MG, (b) MCF-7 and (c) HEK293 cells incubated with blank medium for 4 h (orange) or conjugate **1-RGD** (5 μM, 4 h) before (blue) or after (red) photoirradiation at 450 nm (10 mW cm^{-2}) for 20 min.

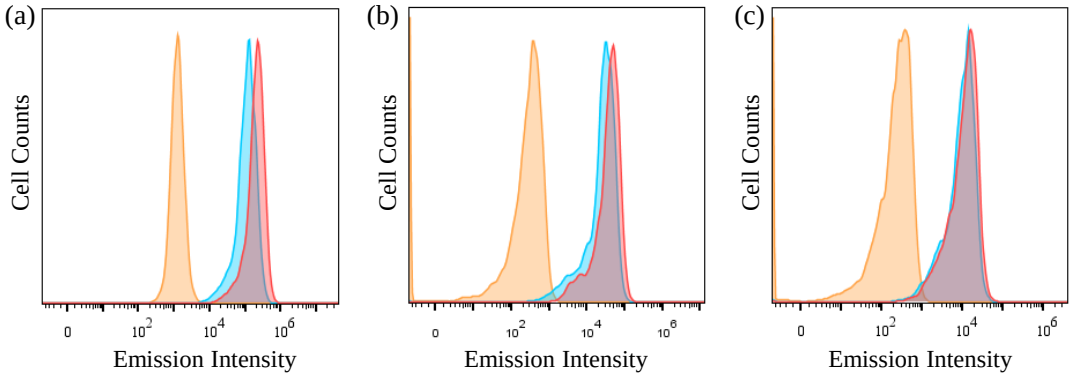

Fig. S10 ESI-mass spectrum of the lysate of U87-MG cells incubated with conjugate **1-RGD** (5 μM, 4 h) followed by photoirradiation at 450 nm (10 mW cm^{-2}) for 20 min.

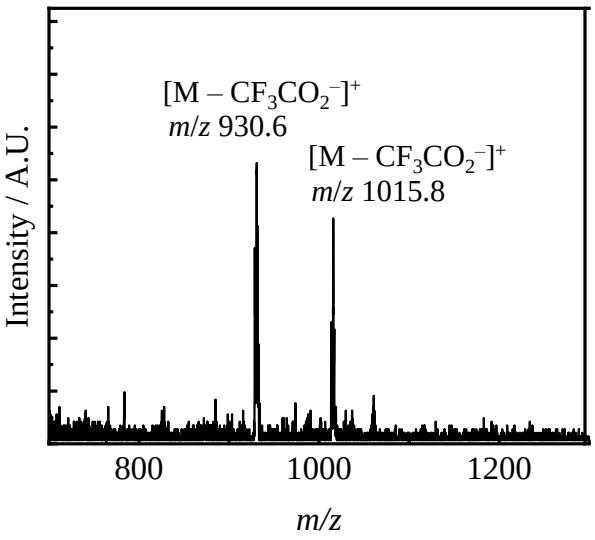

Fig. S11 LSCM images of live U87-MG, MCF-7 and HEK293 cells incubated with complex **2** (5 μM, 4 h; λ_{ex} = 405 nm, λ_{em} = 600 – 700 nm) without (upper) or with (lower) photoirradiation at 450 nm (10 mW cm^{-2}) for 20 min. Scale bar = 20 μm.

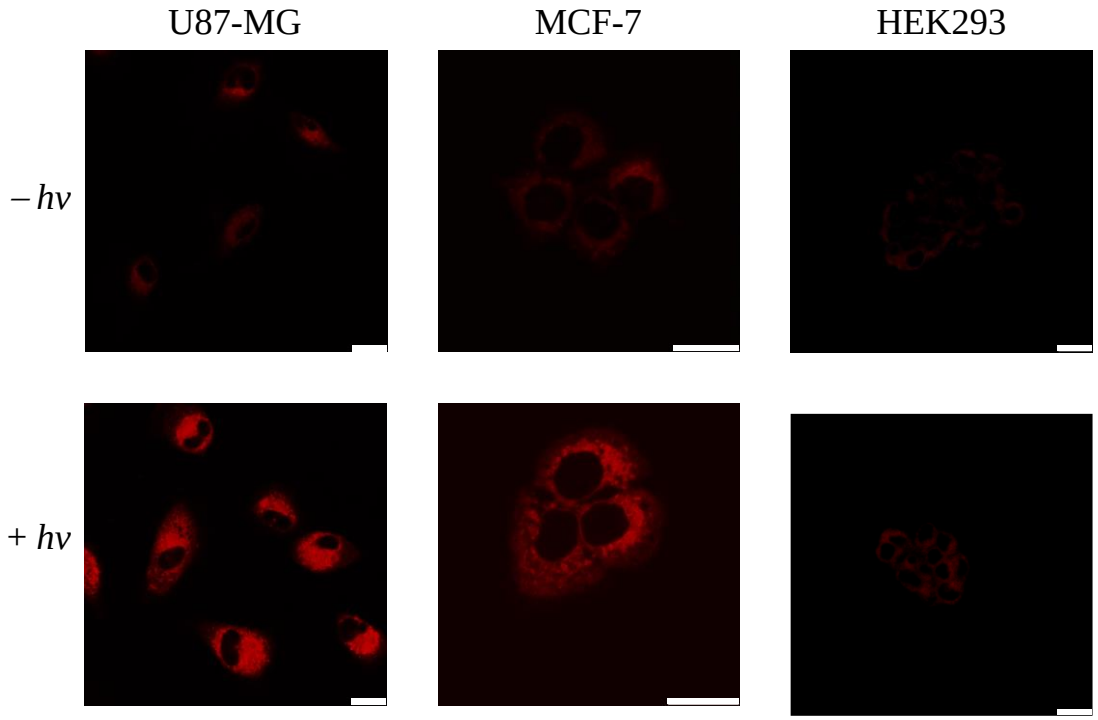

Fig. S12 LSCM images of live U87-MG cells pretreated with conjugate **1-RGD** or complex **2** (5 μM, 4 h; λ_{ex} = 405 nm, λ_{em} = 600 – 700 nm) and then treated with BCN-OH (250 μM, 4 h) followed by incubation with MitoTracker Deep Red (100 nM, 20 min; λ_{ex} = 635 nm, λ_{em} = 650 – 680 nm). Scale bar = 20 μm. Pearson's correlation coefficient (PCC) = 0.96 (**1-RGD**) and 0.97 (**2**).

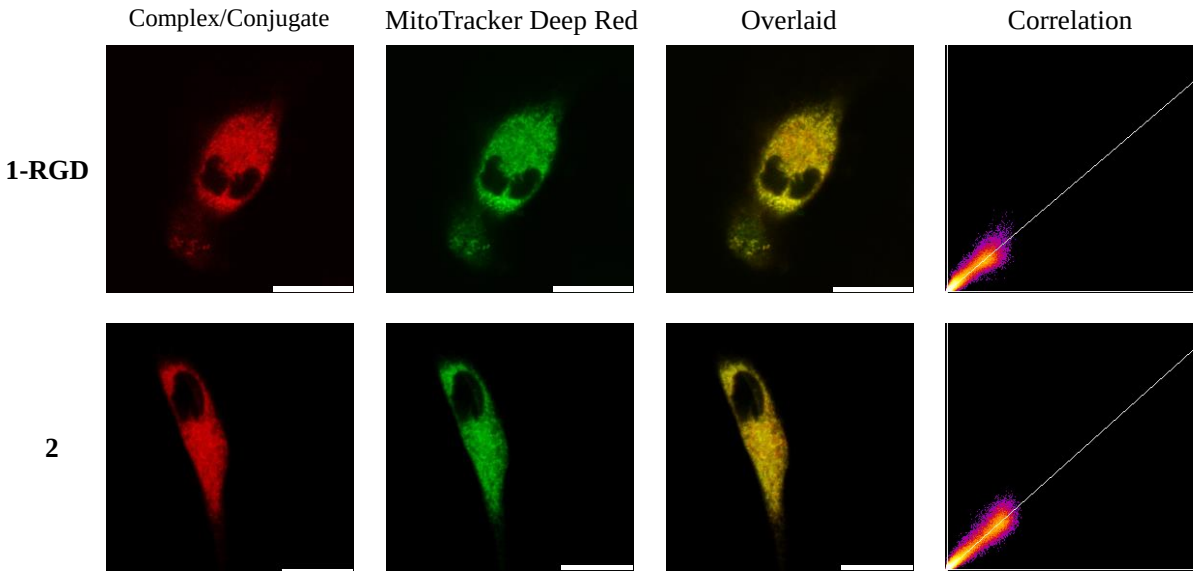

Fig. S13 LSCM images of live/dead cell staining of **1-RGD**-pretreated (5 μM, 4 h) U87-MG cells without (upper) or with (lower) continuous photoirradiation at 450 nm (10 mW cm^{-2}) for 20 min, followed by incubation with Calcein-AM (1 μM, 1 h; λ_{ex} = 488 nm, λ_{em} = 500 – 520 nm) and propidium iodide (10 μM, 1 h; λ_{ex} = 532 nm, λ_{em} = 600 – 650 nm). Scale bar = 20 μm.

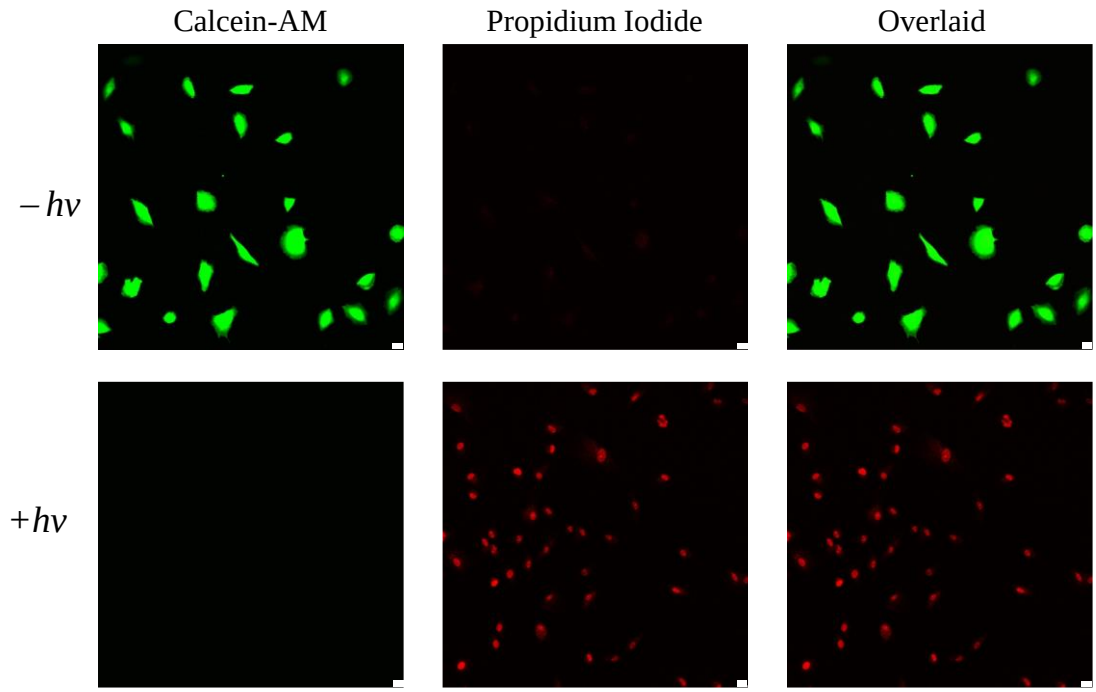

Fig. S14 LSCM images of intracellular ROS of U87-MG cells pretreated with conjugate **1-RGD** (5 μM, 4 h) (a) without or (b) with photoirradiation at 450 nm (10 mW cm^{-2}) for 20 min and further incubation with CM-H_2DCFDA (5 μM, 30 min; λ_{ex} = 488 nm, λ_{em} = 500 – 550 nm). Scale bar = 20 μm.

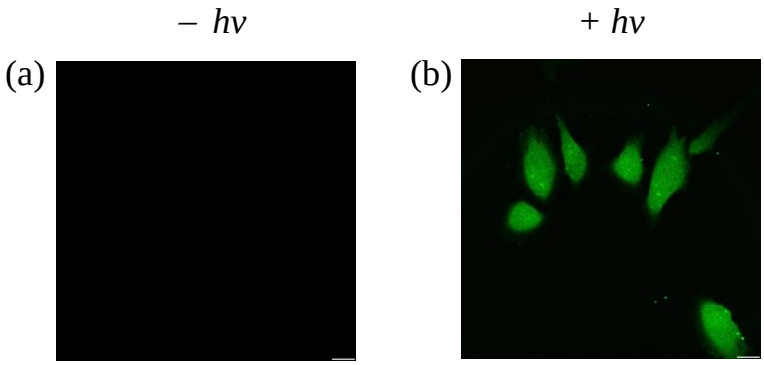

Fig. S15 ^{1}H NMR spectrum of bpy-CONH-SH in DMSO-d_6 at 298 K.

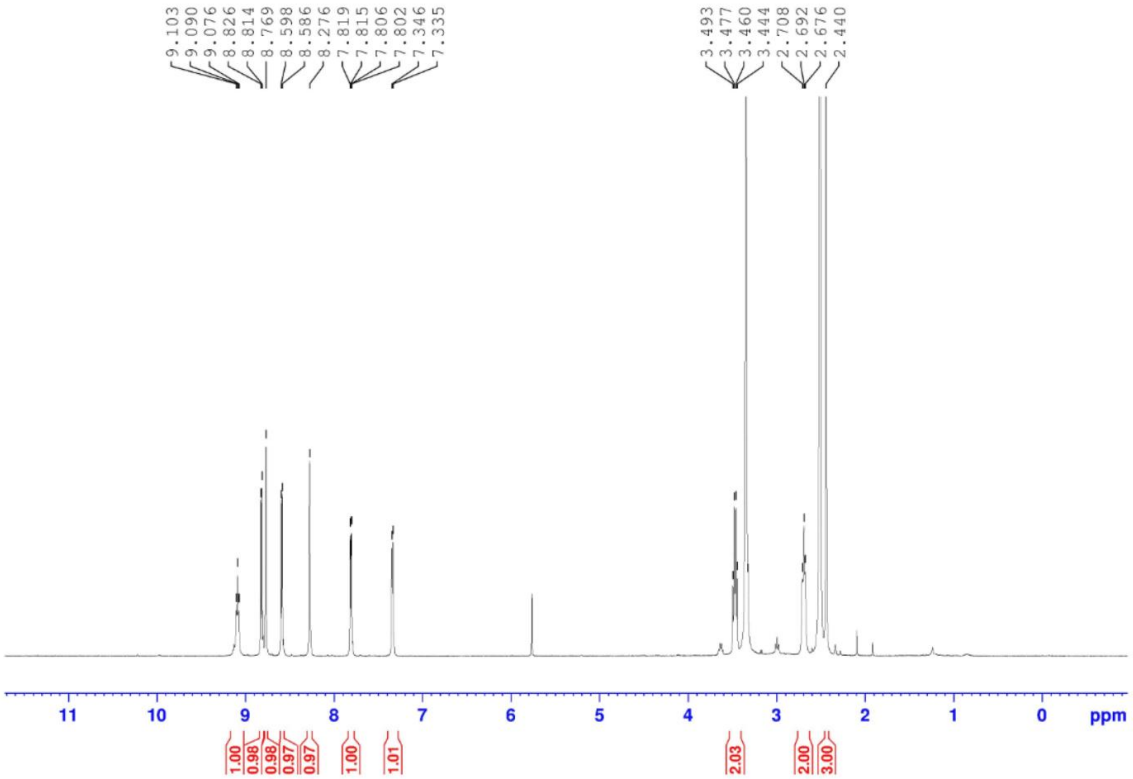

Fig. S16 ^{1}H NMR spectrum of bpy-CONH-S-Tz-Cl in DMSO-d_6 at 298 K.

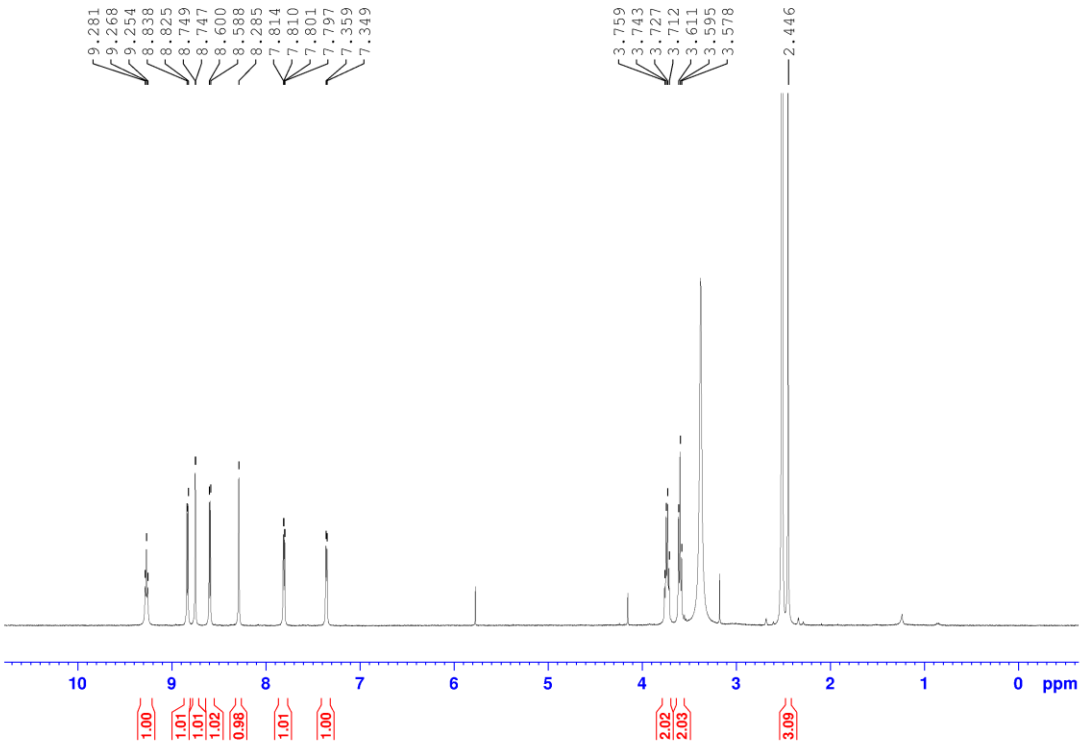

Fig. S17 ^{1}H NMR spectrum of bpy-CONH-S-Tz-S-Et in DMSO-d_6 at 298 K.

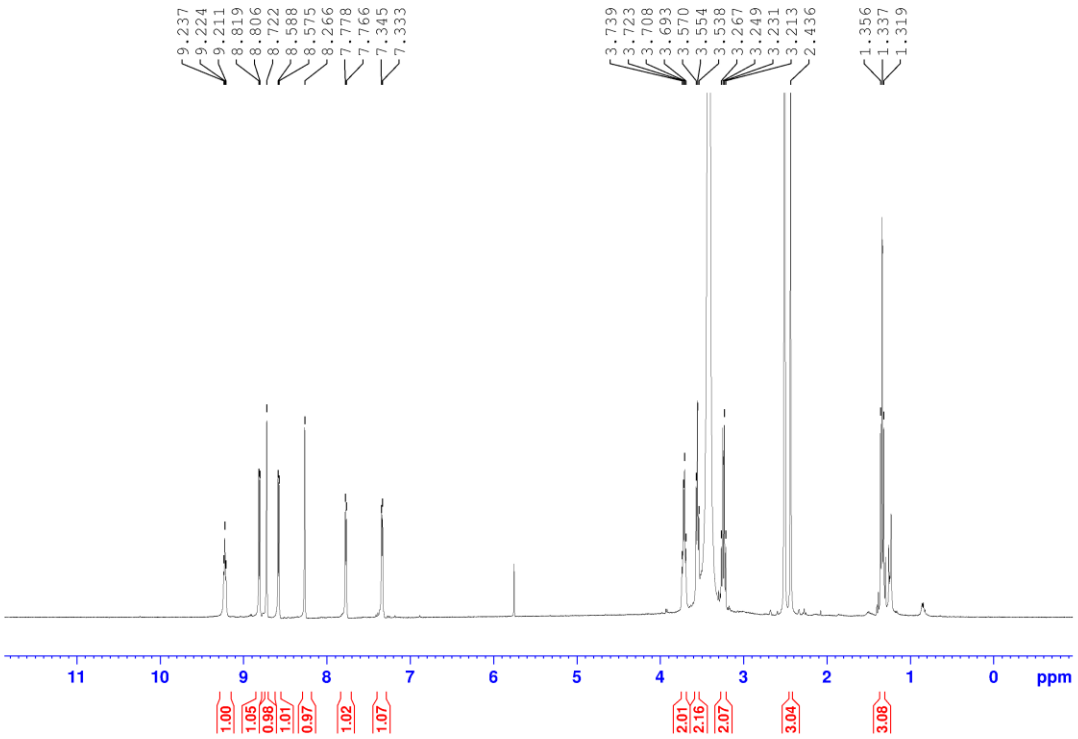

Fig. S18 ^{1}H NMR spectrum of bpy-CONH-SCN in DMSO-d_6 at 298 K.

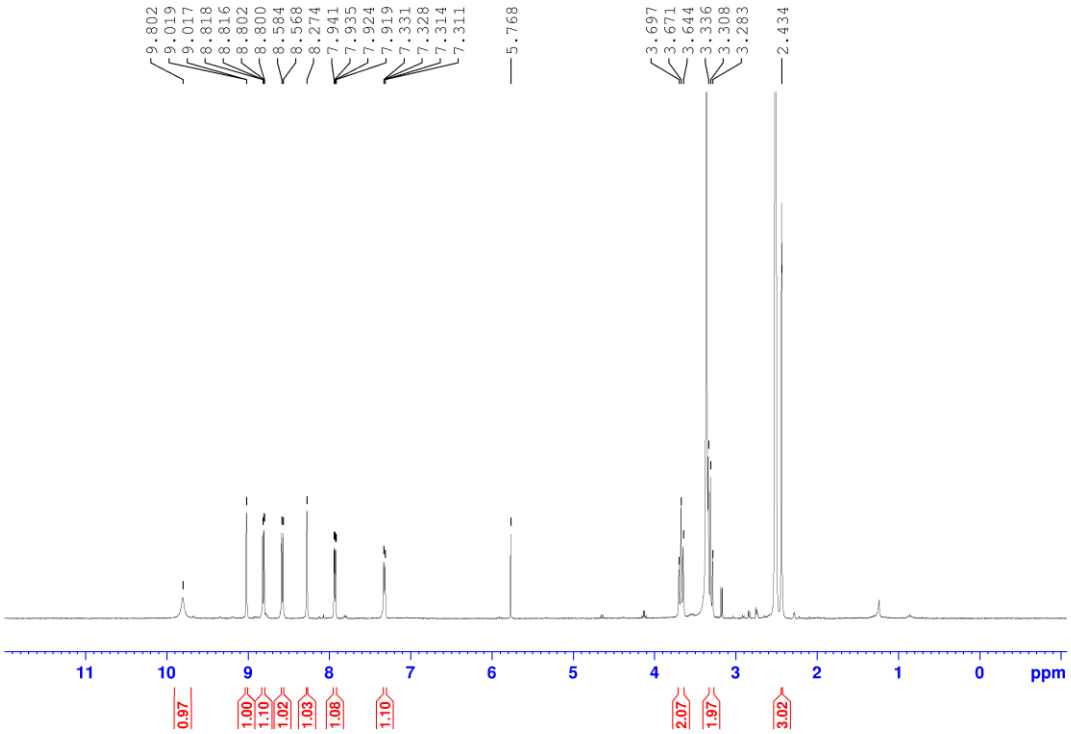

Fig. S19 ^{1}H NMR spectrum of bpy-CONH$_2$ in DMSO-d_6 at 298 K.

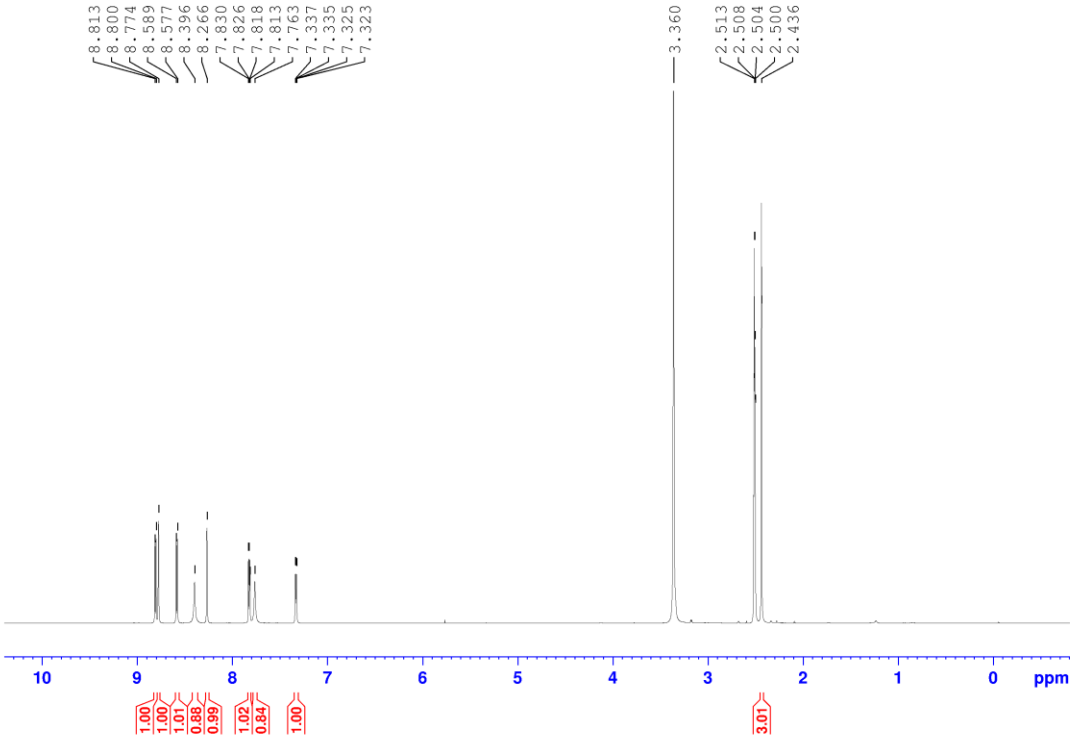

Fig. S20 ^{1}H NMR spectrum of complex **1** in DMSO-d_6 at 298 K.

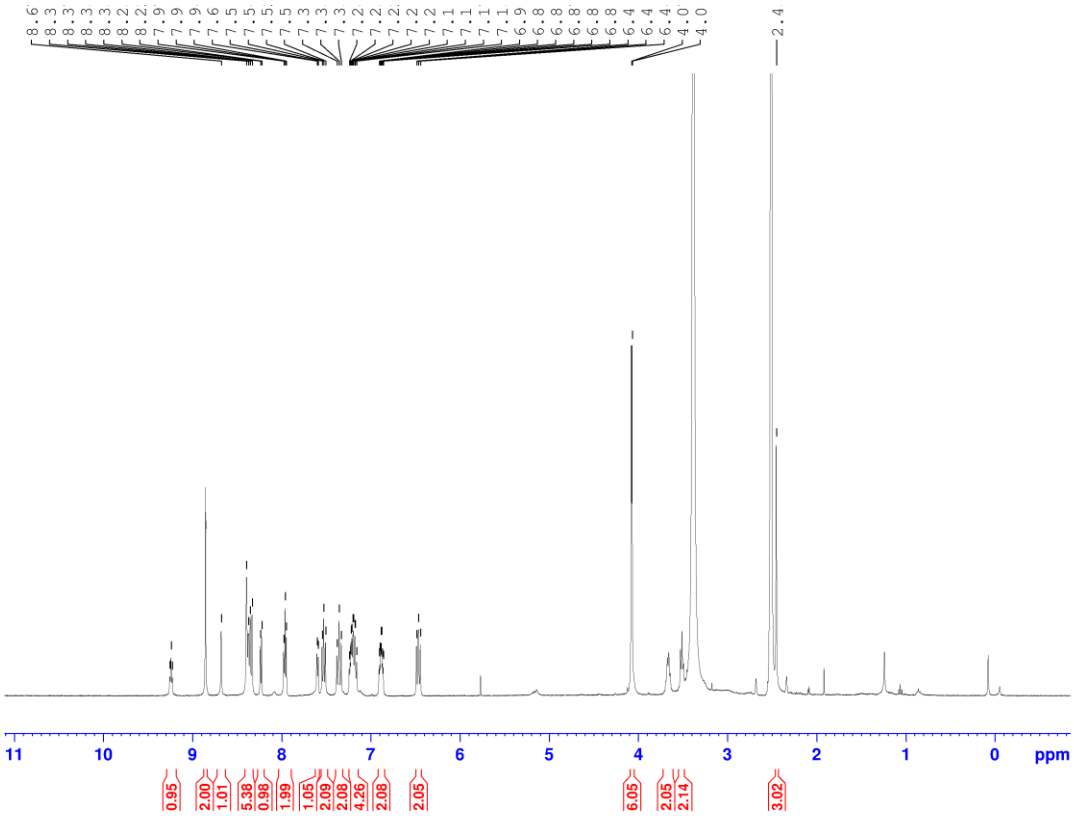

Fig. S21 ^{13}C NMR spectrum of complex **1** in DMSO-d_6 at 298 K.

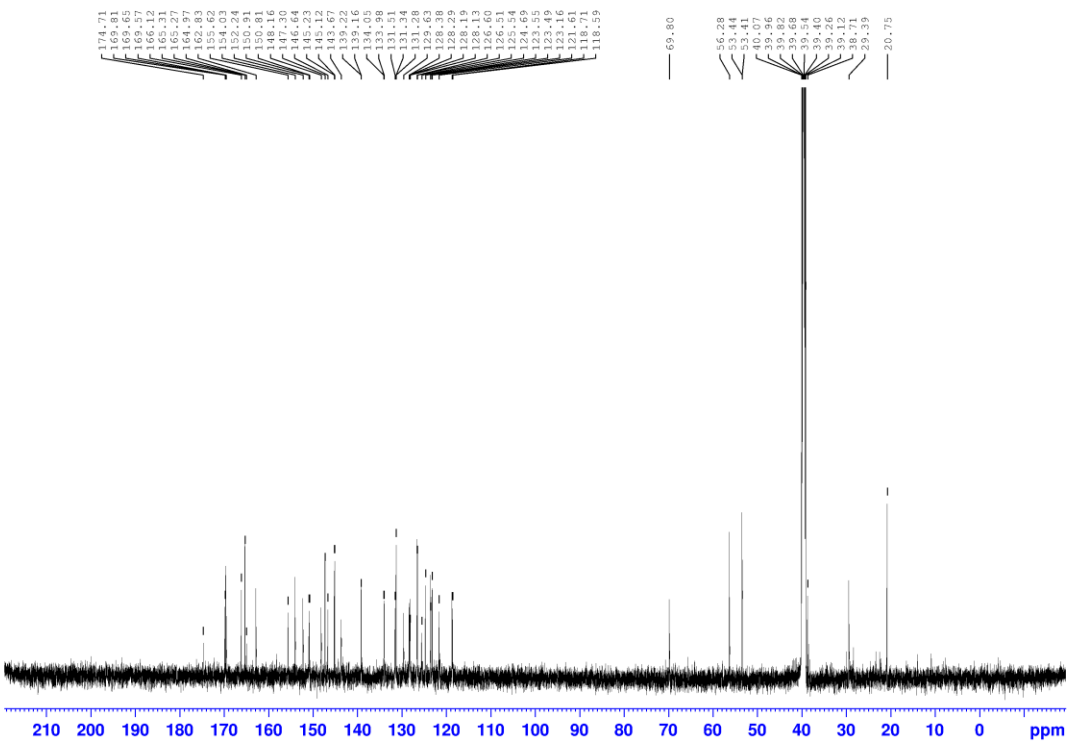

Fig. S22 HR-ESI mass spectra of complex **1** in CH_3CN.

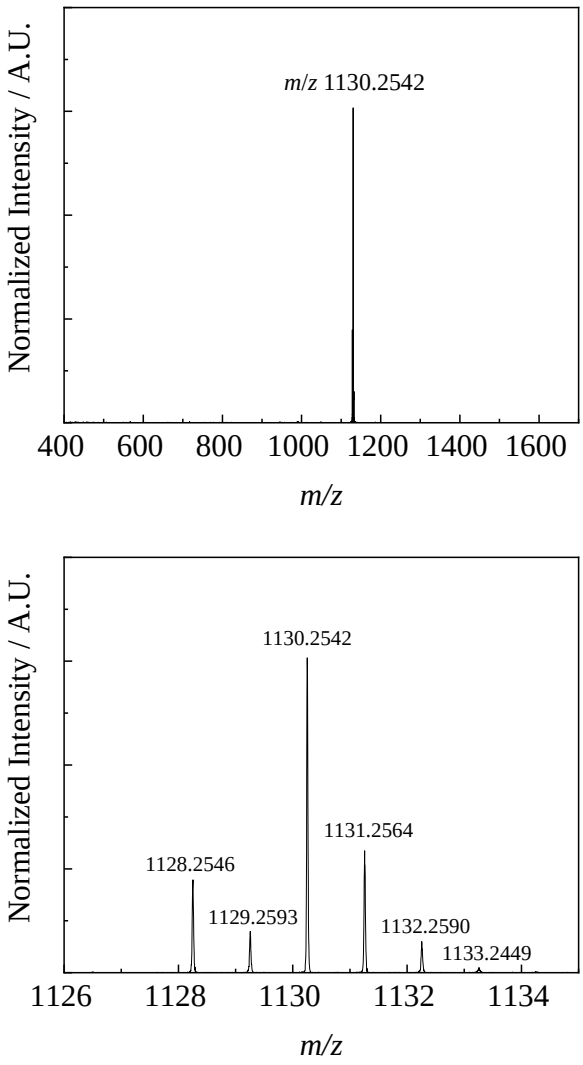

Fig. S23 ^{1}H NMR spectrum of complex **2** in DMSO-d_6 at 298 K.

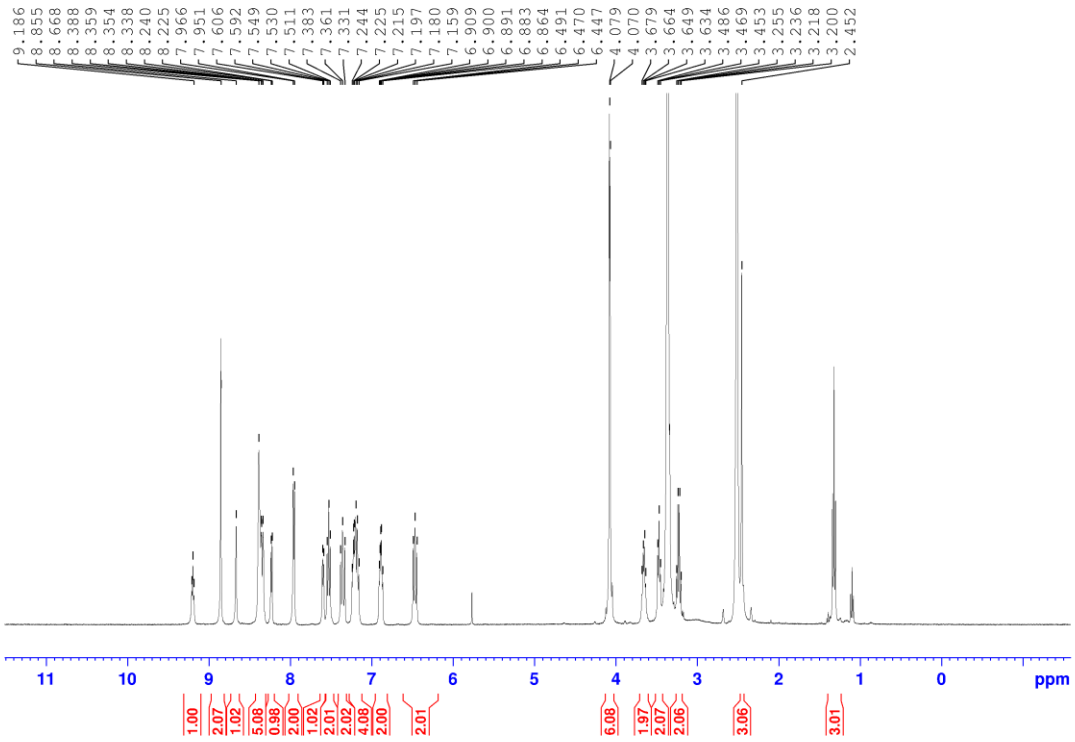

Fig. S24 ^{13}C NMR spectrum of complex **2** in DMSO-d_6 at 298 K.

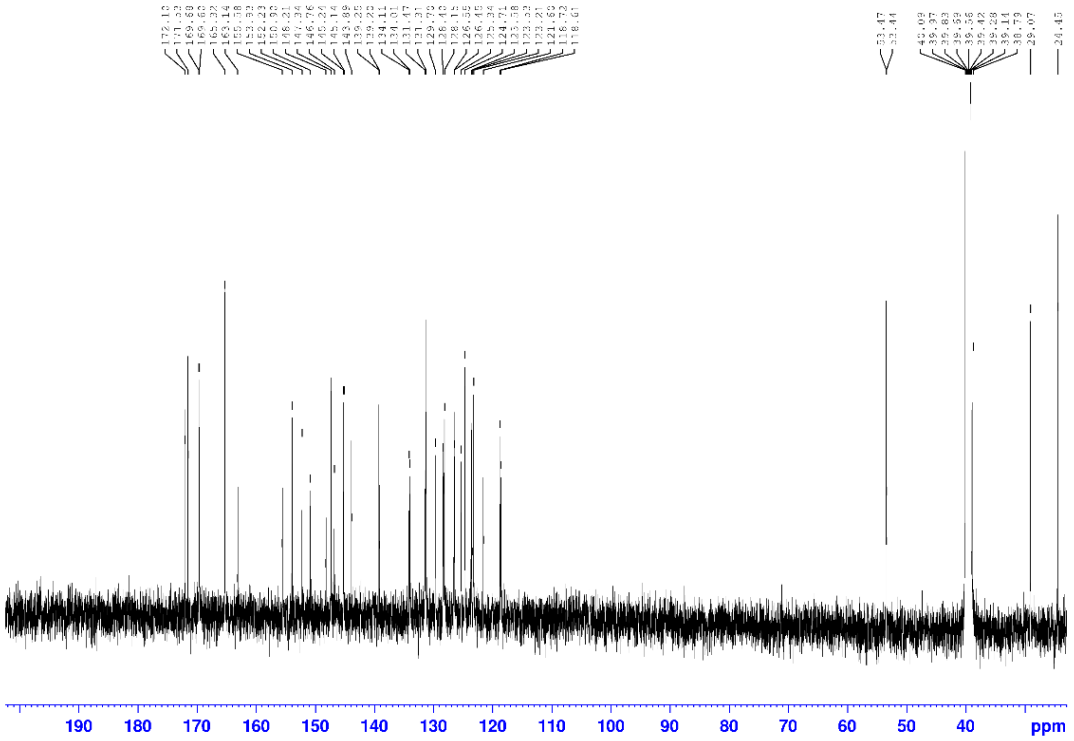

Fig. S25 HR-ESI mass spectra of complex **2** in CH_3CN.

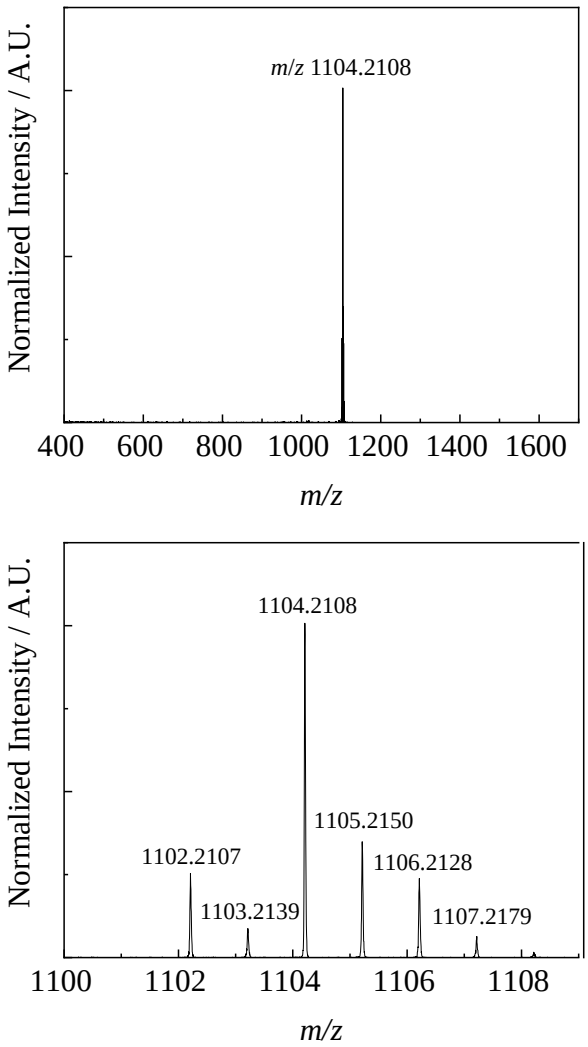

Fig. S26 ^{1}H NMR spectrum of complex **3** in DMSO-d_6 at 298 K.

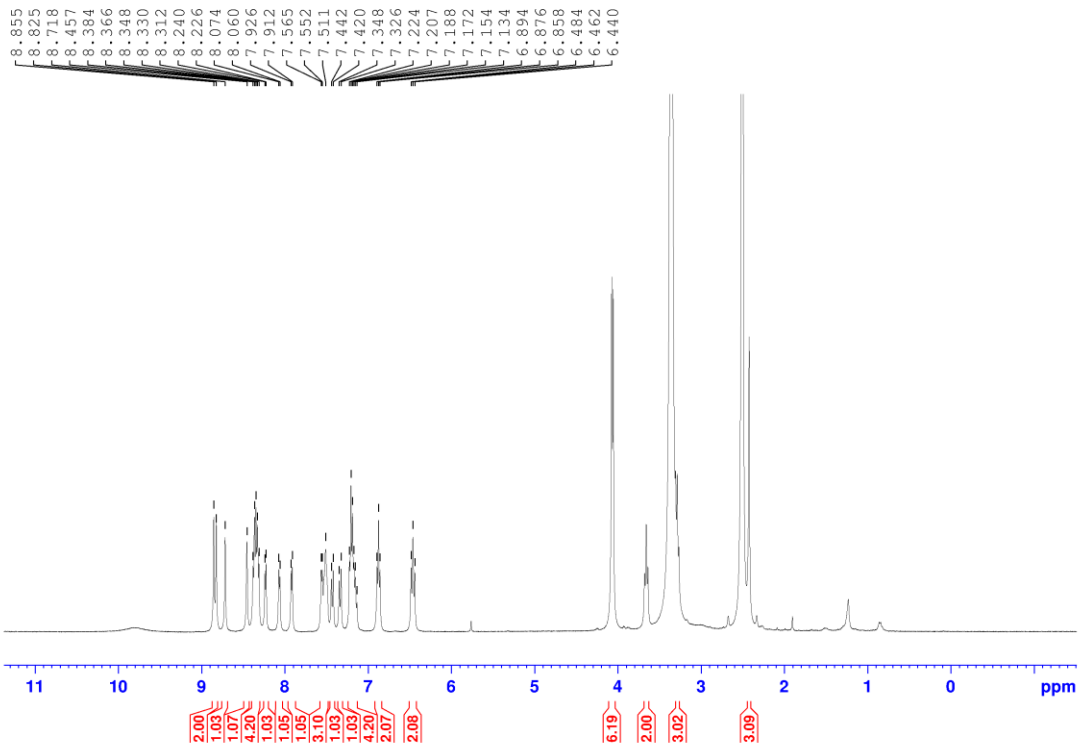

Fig. S27 ^{13}C NMR spectrum of complex **3** in DMSO-d_6 at 298 K.

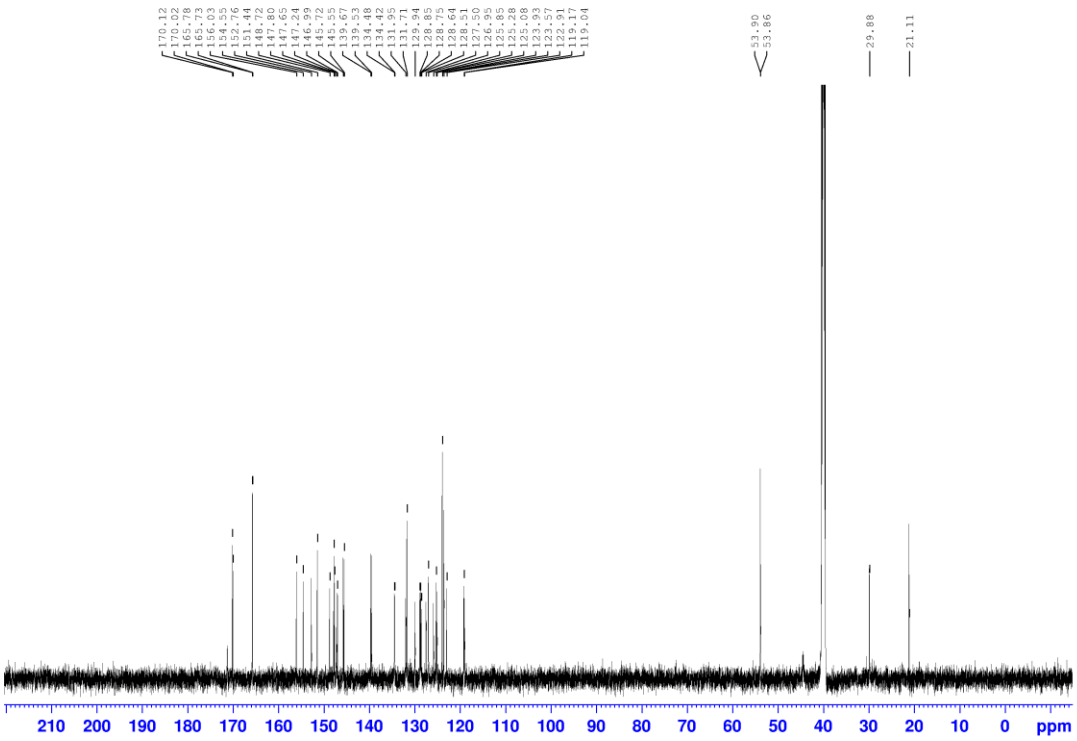

Fig. S28 HR-ESI mass spectra of complex **3** in CH_3CN.

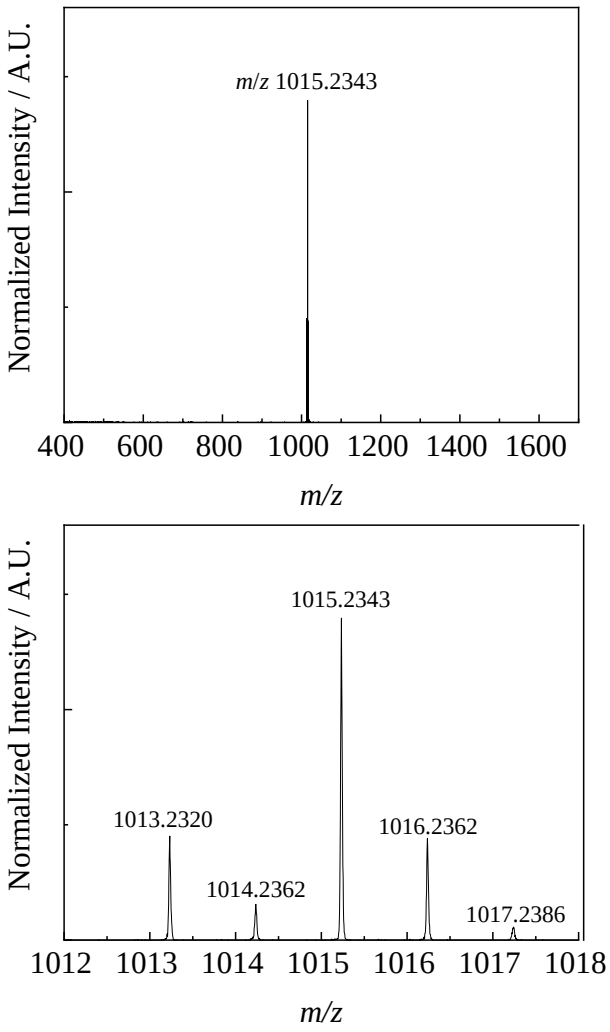

Fig. S29 ^{1}H NMR spectrum of complex **4** in DMSO-d_6 at 298 K.

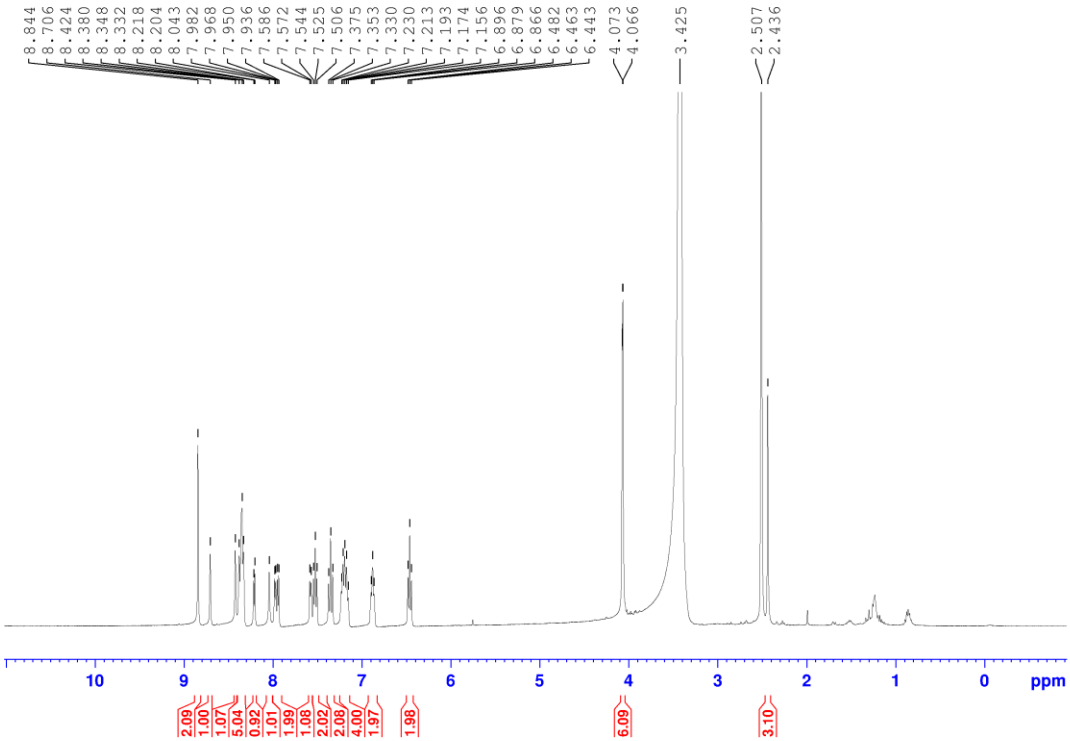

Fig. S30 ^{13}C NMR spectrum of complex **4** in DMSO-d_6 at 298 K.

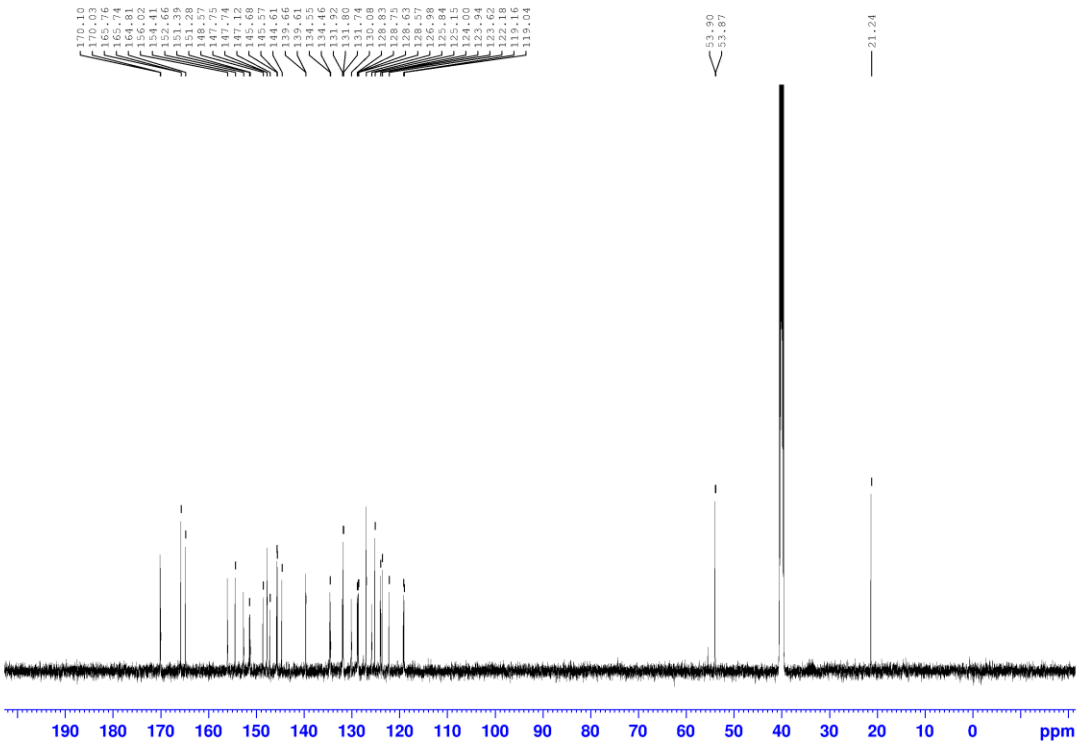

Fig. S31 HR-ESI mass spectra of complex **4** in CH_3CN.

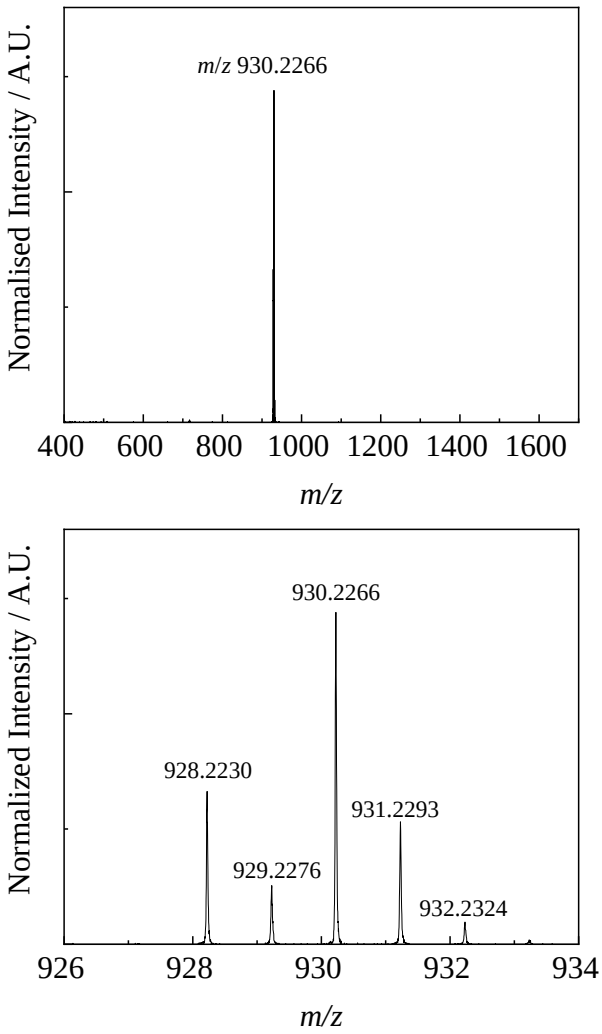

References

1. W. L. F. Armarego, C. Chai, *Purification of Laboratory Chemical*, 7th ed, Butterworth-Heinemann, Oxford, 2013, pp. 103 – 554.
2. T. S.-M. Tang, K.-K. Leung, M.-W. Louie, H.-W. Liu, S. H. Cheng and K. K.-W. Lo, *Dalton Trans.*, 2015, **44**, 4945.
3. B. Koronkiewicz, J. Swierk, K. Regan and J. M. Mayer, *J. Am. Chem. Soc.*, 2020, **142**, 12106.
4. S. Sprouse, K. A. King, P. J. Spellane and R. J. Watts, *J. Am. Chem. Soc*., 1984, **106**, 6647.
5. K. Suzuki, A. Kobayashi, S. Kaneko, K. Takehira, T. Yoshihara, H. Ishida, Y. Shiina, S. Oishi and S. Tobita, *Phys. Chem. Chem. Phys.*, 2009, **11**, 9850.
6. M. Martínez-Alonso, N. Busto, L. D. Aguirre, L. Berlanga, M. C. Carrión, J. V. Cuevas, A. M. Rodríguez, A. Carbayo, B. R. Manzano, E. Ortí, F. A. Jalón, B. García and G. Espino, *Chem. Eur. J.*, 2018, **24**, 17523.
7. A. A. Abdel-Shafi, P. D. Beer, R. J. Mortimer and F. Wilkinson, *J. Phys. Chem. A*, 2000, **104**, 192.
8. M. Forkink, J. A. M. Smeitink, R. Brock, P. H. G. M. Willems and W. J. H. Koopman, *Biochim. Biophys. Acta*, 2010, **1797**, 1034.
9. X. Gong, Y. Didan, J. G. Lock and S. Strömblad, *EMBO J*., 2018, **37**, e98994.
10. L. C. Crowley, B. J. Marfell and N. J. Waterhouse, *Cold Spring Harb. Protoc.,* 2016, **2016**, 778.
11. N.-E. L. Saris, V. V. Teplova, I. V. Odinokova and T. S. Azarashvily, *Anal. Biochem.,* 2004, **328**, 109.